(2)

Semiannual Technical Report

Nitride Semiconductors for Ultraviolet Detection

Supported under Grant #N00014-92-J-1720
Office of the Chief of Naval Research
Report for the period July 1, 1993–December 31, 1993

R. F. Davis, K. Gruss, D. Hanser, B. Perry, L. Smith,
C. Wang and W. Weeks
Materials Science and Engineering Department
North Carolina State University
Campus Box 7907
Raleigh, NC 27695-7907

December, 1993

REPORT DOCUMENTATION PAGE

Form Approved
OMB No. 0704-0188

1. AGENCY USE ONLY (Leave blank)	2. REPORT DATE	3. REPORT TYPE AND DATES COVERED
	December, 1993	Semiannual Technical 7/1/93–12/31/93

4. TITLE AND SUBTITLE

Nitride Semiconductors for Ultraviolet Detection

5. FUNDING NUMBERS

s400018srr01
1114SS
N00179
N66005
4B855

6. AUTHOR(S)

Robert F. Davis

7. PERFORMING ORGANIZATION NAME(S) AND ADDRESS(ES)

North Carolina State University
Hillsborough Street
Raleigh, NC 27695

8. PERFORMING ORGANIZATION REPORT NUMBER

N00014-92-J-1720

9. SPONSORING/MONITORING AGENCY NAMES(S) AND ADDRESS(ES)

Sponsoring: ONR, Code 314, 800 N. Quincy, Arlington, VA 22217-5660
Monitoring: Office of Naval Research Resider
The Ohio State University Research Center
1960 Kenny Road
Columbus, OH 43210-1063

10. SPONSORING/MONITORING AGENCY REPORT NUMBER

11. SUPPLEMENTARY NOTES

12a. DISTRIBUTION/AVAILABILITY STATEMENT

Approved for Public Release; Distribution Unlimited

12b. DISTRIBUTION CODE

13. ABSTRACT (Maximum 200 words)

Monocrystalline thin films of AlN and GaN have been deposited on vicinal alpha(6H)-SiC(0001) wafers via gas-source MBE and cold-wall metalorganic (MO) CVD and extensively investigated via high-resolution TEM. Elemental metal sources combined with activated nitrogen generated using an ECR plasma were employed in the MBE system; triethylgallium, triethylaluminum and ammonia were used in the MOCVD system. The MBE research has also included n-(Si) and p-type(Mg) doping and the creation of p-n junctions. The effects on growth of T, P and MO flux have been investigated in the MOCVD work. Below the critical thickness, AlN only contains threading dislocations emanating from the misfit dislocations; above this thickness, defects parallel to the growth surface greatly increase. The defect density of AlN grown on SiC at 1100°C is much lower than that contained in materials deposited at 700°C. Deposition of GaN on an AlN buffer layer previously deposited on sapphire or SiC results in a larger number of dislocations parallel to the growth surface. A system for the deposition of InN and its solid solutions which addresses the problems of the low decomposition pressure has also been designed. The feasibility of designing an ammonia cracker cell for the MBE system to provide an alternative source of activated nitrogen is being investigated. Microelectronic and optoelectronic device designs have been produced and device-related activities including contact studies involving Zn/Au and Cr/Au and Au, reactive ion etching and optical characterization have been initiated.

14. SUBJECT TERMS

GaN, AlN, InN, thin films, metalorganic chemical vapor deposition (MOCVD), molecular beam epitaxy (MBE), TEM, ECR plasma, Mg doping, p-n junctions, contacts, reactive ion etching (RIE), optical characterization

15. NUMBER OF PAGES

52

16. PRICE CODE

17. SECURITY CLASSIFICATION OF REPORT	18. SECURITY CLASSIFICATION OF THIS PAGE	19. SECURITY CLASSIFICATION OF ABSTRACT	20. LIMITATION OF ABSTRACT
UNCLAS	UNCLAS	UNCLAS	SAR

Table of Contents

I. Introduction

Continued development and commercialization of optoelectronic devices, including light-emitting diodes and semiconductor lasers produced from III–V gallium arsenide-based materials, has also generated interest in the much wider bandgap semiconductor mononitride materials containing aluminum, gallium, and indium. The majority of the studies have been conducted on pure gallium nitride thin films having the wurtzite structure, and this emphasis continues to the present day. Recent research has resulted in the fabrication of p–n junctions in wurtzitic gallium nitride, the deposition of cubic gallium nitride, as well as the fabrication of multilayer heterostructures and the formation of thin film solid solutions. Chemical vapor deposition (CVD) has usually been the technique of choice for thin film fabrication. However, more recently these materials have also been deposited by plasma-assisted CVD and reactive and ionized molecular beam epitaxy.

The program objectives in this reporting period have been (1) the investigation of the defects generated during the growth of GaN and AlN on SiC(0001) and sapphire, (2) the use of MOCVD to grow AlN, GaN and InN thin films, (3) the design of a MOCVD system for deposition of InN and InN alloy films, (4) the development of facilities for the deposition of ohmic and rectifying contacts, reactive ion etching and photo- and cathodoluminescence for III-V materials and (5) design of microelectronic devices.

The procedures, results, discussions of these results and conclusions of these studies are summarized in the following sections with reference to appropriate SDIO/ONR reports for details. Note that each major section is self-contained with its own figures, tables and references.

II. Metalorganic Chemical Vapor Deposition (MOCVD) of III-V Nitrides

A. Introduction

The potential semiconductor and optoelectronic applications of the III-V nitrides has prompted significant research in thin film growth and development. The materials of concern in this section are AlN and GaN, specifically, with InN and layered nitrides receiving some attention. Because GaN in the wurtzite structure with a bandgap of 3.4 eV [1] forms continuous solid solutions with both AlN and InN, for example, which have bandgaps of 6.2 eV [2] and 1.9 eV [3], respectively, engineered bandgap materials could result in optoelectronic devices active from the visible to deep UV frequencies [4].

For growing III-V nitrides Metalorganic Chemical Vapor Deposition (MOCVD) has presently gained favor over Atomic Layer Epitaxy (ALE) and layer-by-layer approaches because of the desire to have higher growth rates. CVD also offers higher deposition temperatures beneficial in improving growth characteristics. Thus, a fully operational cold-wall vertical barrel MOCVD reactor system has been built. GaN, AlN, InN, their solid solutions, graded layer structures and heterostructures can be grown. The CVD system also has the capabilities for introducing p- and n-type dopants for incorporation into the growing thin films.

Experimental procedures, results to date, conclusions and plans for future work will be included here.

B. Experimental Procedure

For growing the III-V nitrides the gallium, aluminum and indium sources are triethylgallium (TEG)[$Ga(C_2H_5)_3$], triethylaluminum (TEA)[$Al(C_2H_5)_3$] and trimethylindium (TMI)[$In(CH_3)_3$], respectively, installed in the familiar bubbler arrangement with nitrogen used as the carrier gas. TE(G,A) was chosen over TM(G,A) because of its lower decomposition temperature range and a lower carbon incorporation in the growing film during surface decomposition reactions [4]. However, for InN deposition TMI is the organometallic of choice. This results because the TEI precursor is much less thermally stable than its methyl counterpart and undergoes appreciable decomposition starting at 40°C [5] as compared to 270-300°C for TMI [6-9]. Ammonia (NH_3) is used as the nitrogen source. The system is also equipped with an n-type dopant species, silane (SiH_4) 8.2 ppm in N_2, and a p-type dopant organometallic species, bis-cyclopentadienyl magnesium (Cp_2Mg)[$Mg(C_5H_5)_2$], with nitrogen as its carrier gas.

Substrates generally used are α(6H)-SiC (0001) 3° off-axis toward [$11\bar{2}0$]. These SiC wafers are received with a thin (~ 750Å) surface oxide layer. The wafers are cleaned in a 10% HF solution, dried and immediately loaded into the load lock and onto a SiC-coated

graphite susceptor. With the diffusion pump, base pressures near 1×10^{-5} torr are reached before deposition begins. The CVD system schematic is included below to better illustrate the system's features and capabilities, see Fig. 1.

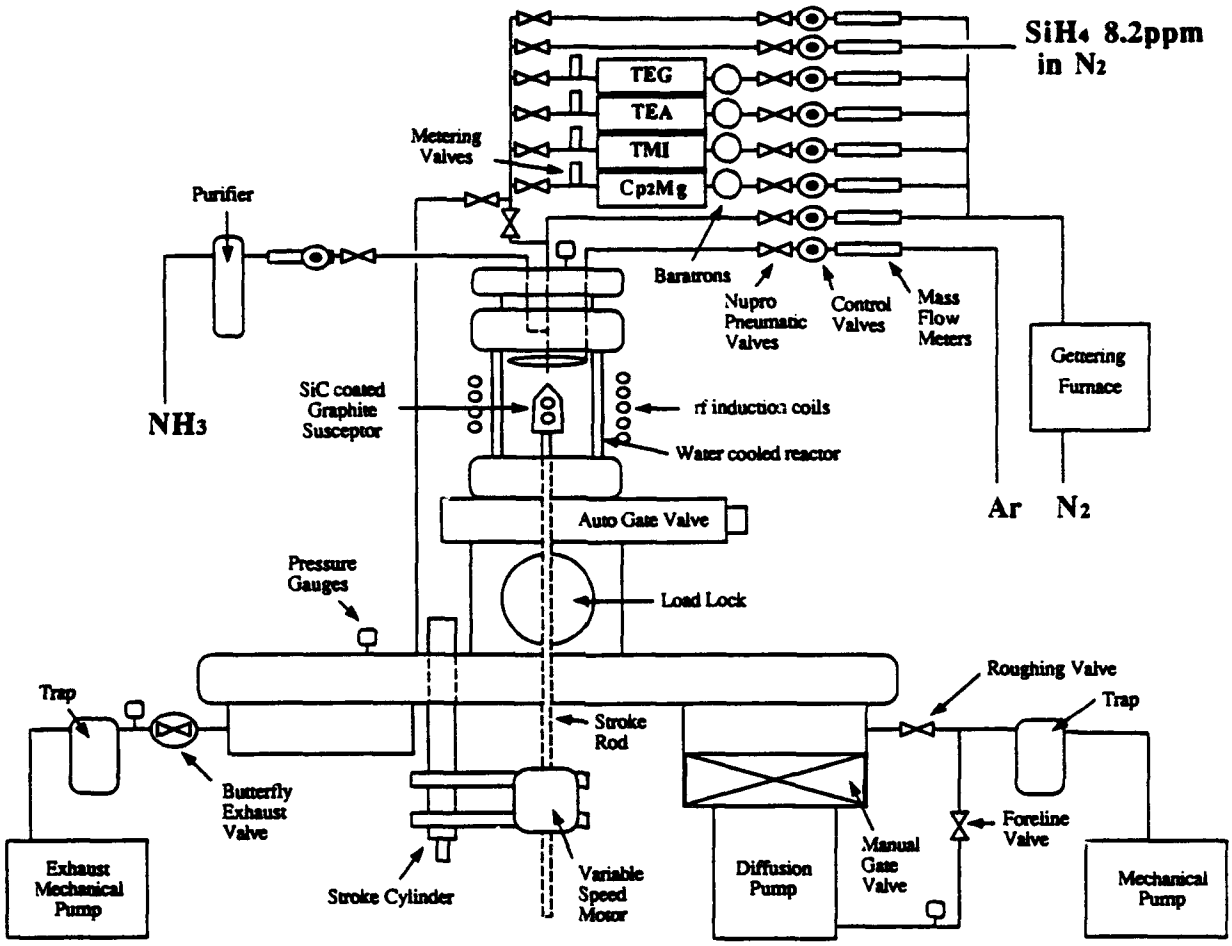

Figure 1. CVD System Schematic.

Once the required base pressure is reached, the manual gate valve to the diffusion pump is closed. With the butterfly exhaust valve controller in the auto mode and the desired run pressure dialed in, the N_2 diluent and Ar curtain-ring gases are ramped up to their preset flow rates. The inert argon curtain-ring is used in an effort to retard unwanted deposition on the water-cooled quartz reactor walls. At this time susceptor rotation of approximately 5 rpm begins. As the pressure is equilibrating at the desired level, the rf induction heating power generator is tuned to the proper power setting. The temperature of the susceptor is monitored using a Leeds & Northrup Optical Pyrometer.

Once the setpoint temperature has been reached, the proper bubbler pressures and carrier gas flow rates are established corresponding to the desired amounts of precursor materials. These gases bypass the reactor and are sent directly to "vent" during equilibration.

Simultaneously, the NH_3 is ramped up to its setpoint. Generally, the ammonia flows for only a few seconds before the column-III organometallics and dopants, if applicable, are switched from "vent" to "run." Once the MO precursors are diverted into the reactor chamber film deposition begins.

During growth it is imperative to monitor gas flow rates, cooling water flow and susceptor temperature to help improve growth uniformity. Once the desired deposition time has elapsed, the run is terminated in reverse order. The column-III precursors (and dopants) are switched off, as is the rf power supply if no post-growth annealing is necessary. Usually the sample remains under flowing NH_3, N_2 and Ar until it cools below approximately 500°C. At this point the NH_3 is switched off and the sample continues to cool under flowing nitrogen and argon for an additional hour and a half. After this length of time, all the gases and cooling water lines can be closed off. The reactor chamber is then evacuated and refilled with argon at least once before removing the sample.

Reflection high-energy electron diffraction (RHEED) was used to investigate the microstructure and crystallinity of the deposited films. Scanning Electron Microscopy (SEM) was employed for observing the surface morphologies and cross-sectional thicknesses of the deposited films.

C. Results

CVD of AlN. Deposition of AlN and attempts at doping have been an area of vigorous research. The parameters of temperature, pressure and TEA flux have been systematically varied while seeking to optimize AlN growth. TEA flow rates of 6.02, 8.03, 11.95 and 17.54 μmol/min have been used to grow AlN samples at 1000°C and a total system pressure of 45 torr. The other variables of interest remained constant throughout the series of these experiments and were as follows: NH_3 flow rate = 1.5 slm, N_2 flow rate = 1.5 slm and Ar curtain-ring flow rate = 1.5 slm. The RHEED patterns of the above described samples varied very little. Each pattern revealed streaky spots and Kikuchi lines. The patterns were indicative of the wurtzite structure and apparently a monocrystalline film. Figures 2 and 3 show typical examples of the MOCVD grown AlN on SiC at 1000°C.

Attempts have been made to p-type dope AlN using the magnesium source, Cp_2Mg. Two samples with TEA flow rates of 8.03 μmol/min and 17.54 μmol/min, respectively, with all other variables the same as listed above have been grown at 1000°C and 45 torr. The Cp_2Mg flow rate was 1.19 μmol/min for each run. After terminating the TEA and Cp_2Mg flows, the NH_3 flow was also switched off, but the susceptor was kept at temperature (i.e. 1000°C) for an additional ten minutes in flowing N_2 and Ar. Recall, this is not the same procedure for cooling undoped samples. The samples were annealed in a non-hydrogen environment in an effort to liberate any incorporated hydrogen atoms in the film that may be tying up the p-type

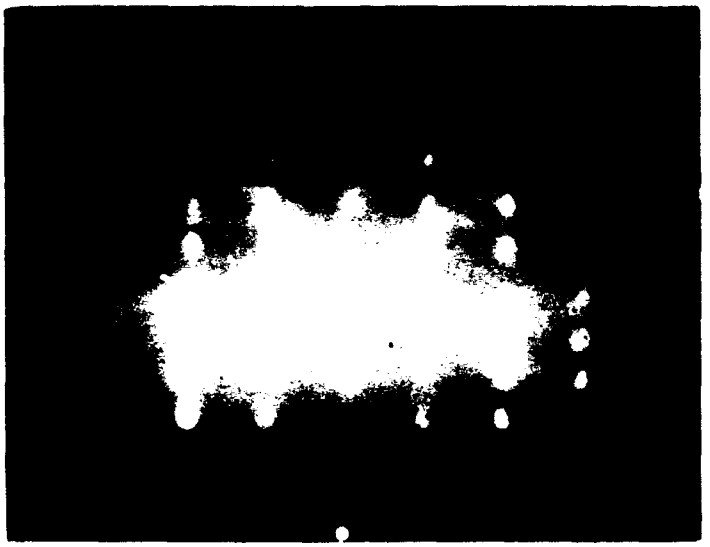

[$2\bar{1}\bar{1}0$] Azimuth

Figure 2. RHEED pattern for AlN deposited on α(6H)-SiC at 1000°C. TEA flow rate was 8.03 μmol/min.

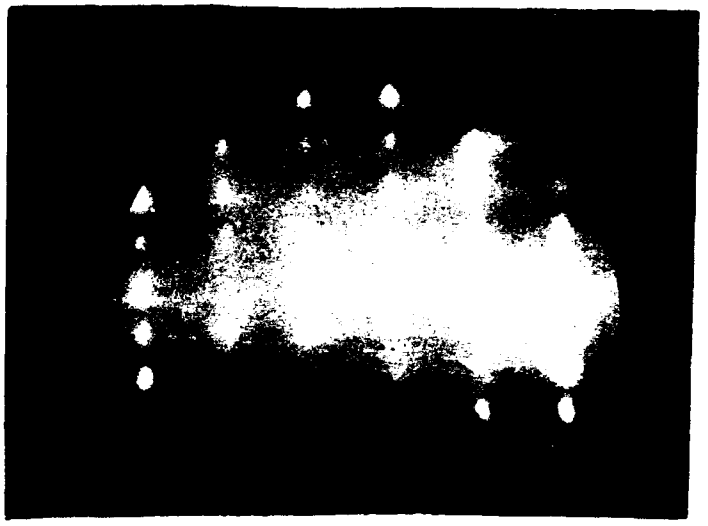

[$2\bar{1}\bar{1}0$] Azimuth

Figure 3. RHEED pattern for AlN deposited on α(6H)-SiC at 1000°C. TEA flow rate was 17.54 μmol/min.

acceptors. In a global effort to minimize the amount of hydrogen entering the growth reactor, nitrogen and not the usual hydrogen is used as the diluent gas, the carrier gases and also as the balance gas in the very dilute concentration of silane. Hall mobility measurements and carrier concentration determinations of these doped films are forthcoming.

Other attempts at growing AlN have been conducted at 1100°C and 45 torr. To date, TEA flow rates of 8.03, 11.95 and 17.54 μmol/min have been used to grow thin films, with all other parameters the same as listed above. Several RHEED images of selected AlN samples grown at 1100°C are shown below, see Figs. 4 and 5.

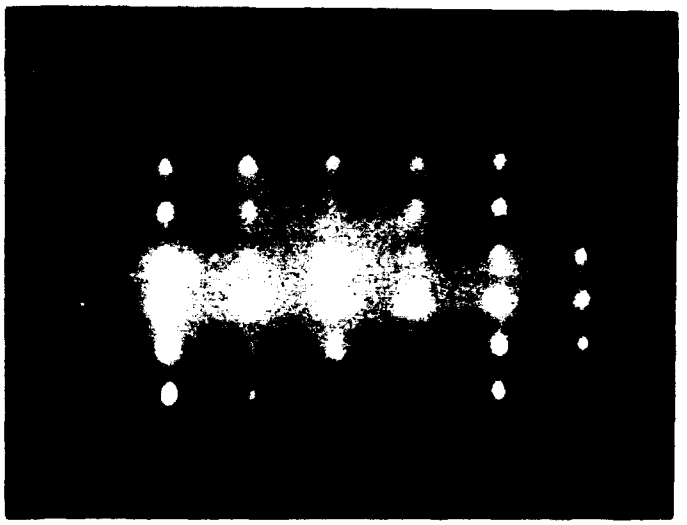

[$2\bar{1}\bar{1}0$] Azimuth

Figure 4. RHEED pattern for AlN deposited on α(6H)-SiC at 1100°C. TEA flow rate was 11.95 μmol/min.

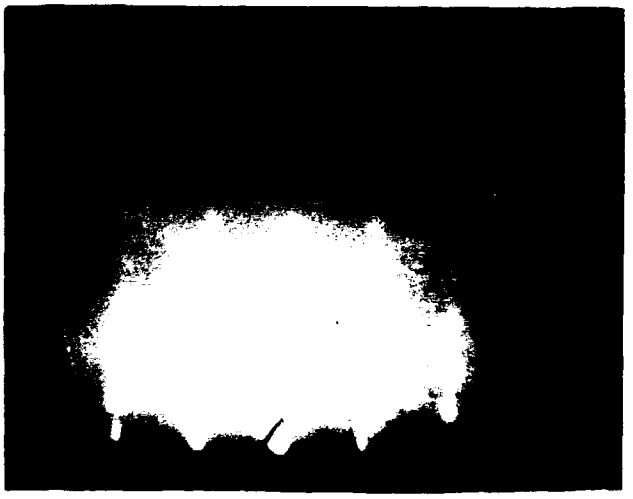

[$2\bar{1}\bar{1}0$] Azimuth

Figure 5. RHEED pattern for AlN deposited on α(6H)-SiC at 1100°C. TEA flow rate was 17.54 μmol/min.

CVD of GaN. Numerous GaN samples have been grown under a wide range of growth parameters. In short, between a total system pressure of between 30 torr and 57 torr, a TEG flow rate of 10.2 μmol/min, NH_3 at 1 slm, N_2 at 1.5 slm and Ar at 100 sccm has produced the best quality films to date. RHEED images of GaN films grown under the above conditions at 30 torr and 57 torr are shown below, see Figs. 6 and 7.

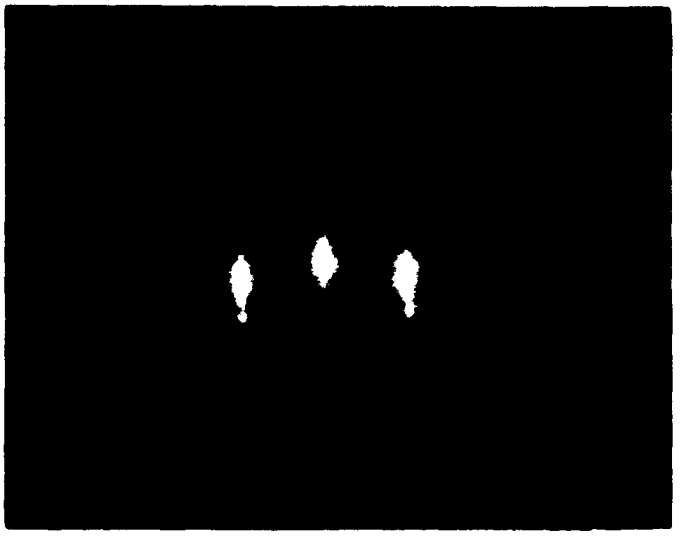

[$2\bar{1}\bar{1}0$] Azimuth

Figure 6. RHEED pattern for GaN deposited on α(6H)-SiC at 1000°C and 30 torr. TEG flow rate was 10.2 μmol/min.

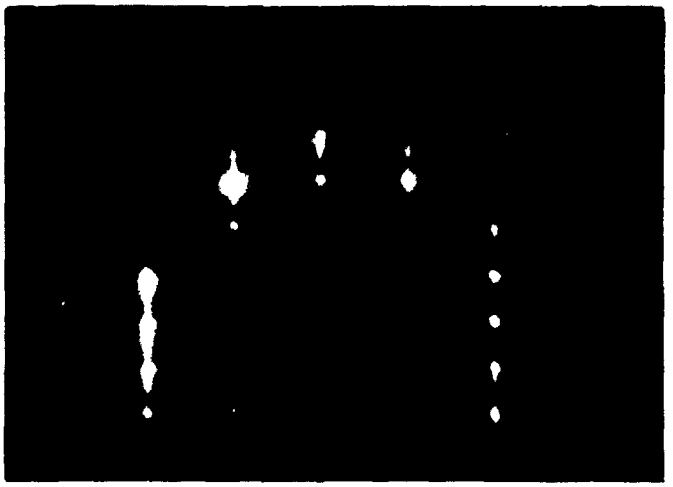

[$2\bar{1}\bar{1}0$] Azimuth

Figure 7. RHEED pattern for GaN deposited on α(6H)-SiC at 1000°C and 57 torr. TEG flow rate was 10.2 μmol/min.

CVD of InN. Attempts at growing InN directly on SiC using the layer-by-layer approach described in a previous report has resulted in only "pools" of indium being deposited. Using the CVD system, attempts were made to deposit InN on both GaN and AlN buffer layers. After a GaN buffer layer was grown at 1000°C and 57 torr, the susceptor was cooled to 800°C and the run pressure was increased to 200 torr. Then the TMI flow rate was set to 12.24 μmol/min with NH_3 and N_2 both set at 1.5 slm. The InN growth period lasted one hour.

Similarly in another experiment, after a AlN buffer layer was grown at 1000°C and 30 torr, the susceptor temperature was cooled to 650°C and the run pressure was again increased to 200 torr. All other InN deposition parameters, except temperature, remained the same as for the GaN buffered film, including deposition time.

Utilizing EDS and AES, virtually no observable InN grown at 800°C was detected on the GaN buffer layer. SEM of this sample showed only a smooth, featureless surface, presumably that of the GaN buffer layer. However, the InN film grown at 650°C on AlN was easily detectable by EDX and also visible via SEM. The SEM micrograph of InN revealed a uniformly faceted, highly oriented surface texture, not unexpected for a growth temperature of 650°C. The facets were approximately 1200Å in size.

D. Discussion

The as-grown AlN films have proven to be very highly resistive. This has caused substantial charging problems when trying to image the surfaces and especially the cross-sectional thicknesses using SEM. Carbon-coating the samples proved to be no help in alleviating the charging problems. Thus, accurate growth rates could not be determined for the various AlN samples grown. Also since cleaving a sample for use in obtaining cross-sectional thickness via SEM is destructive, ellipsometry will begin to be used for determining the thickness of deposited films. Otherwise, using SEM the AlN surfaces appeared uniform and featureless. No faceting was observed.

These high impedance materials, especially AlN, also inhibit the accurate, if any, measuring of Hall mobilities and carrier concentrations. For these reasons, it is imperative that one be able to appreciable dope these materials to improve carrier concentrations, increase mobilities and decrease their resistivities.

For InN growth, two important findings need to be addressed. Firstly, at less than atmospheric pressures it appears that InN can not be grown at temperatures much greater than 650°C. Secondly, at temperatures ≤ 650°C an AlN buffer layer on SiC (or presumably a GaN buffer layer) is a necessary aid for heteroepitaxy of InN on SiC.

E. Conclusions

Apparent monocrystalline AlN and GaN thin films have been grown using a vertical MOCVD reactor system. The AlN was grown at both 1000°C and 1100°C. The GaN was deposited at 1000°C. Also, a highly oriented InN film was deposited on an AlN buffer layer on SiC at 650°C.

F. Future Research Plans/Goals

Investigating the effects on growth upon varying certain deposition parameters such as temperature, pressure, MO flow rate and III/V input ratios will continue in an effort to optimize growth conditions from a microstructural and electrical property point of view.

Deposition of III-V nitride using GaN and/or AlN buffer layers will be attempted. The use of a buffer layer may reduce the effects of lattice mismatch between the SiC substrate and the depositing film and aid in the growth of more desirable, non-faceted, uniformly smooth films.

Because of the highly resistive nature of the nitride films, p- and n-type doping of GaN and especially AlN must be accomplished in order to more accurately measure Hall mobilities and carrier concentrations. Photoluminescence and cathodoluminescence characteristics will also be investigated on future samples. SIMS, in conjunction with Hall measurements, will be used to compare dopant concentrations versus activated majority charge carriers. A grand goal would be to fabricate a simple devices such as a Schottky diode or a pn-junction.

G. References

1. H. P. Maruska and J. J. Tietjen, Appl. Phys. Lett., **15** (1969) 327.
2. W. M. Yim, E. J. Stofko, P. J. Zanzucchi, J. I. Pankove, M. Ettenberg and S. L. Gilbert, J. Appl. Phys., **44** (1973) 292.
3. J. A. Sajurjo, E. Lopez-Cruz, P.Vogh and M. Cardona, Phys. Rev., **B28** (1983) 4579.
4. J. Sumakeris, Z. Sitar, K. S. Ailey-Trent, K. L. More and R. F. Davis, Thin Solid Films, **225** (1993) 244.
5. *CVD Metalorganics for Vapor Phase Epitaxy: Product Guide and Literature Review II*, Advanced Materials, Morton International, Danvers, MA.
6. D. A. Jackson, Jr., J. Crystal Growth, **94** (1989) 459.
7. R. Karlicek, J. A. Long and V. M Donnelly, J. Crystal Growth, **68** (1984) 123.
8. C. A. Larsen and G. B. Stringfellow, J. Crystal Growth, **75** (1986) 247.
9. N. I. Buchan, C. A. Larsen and G. B. Stringfellow, J. Crystal Growth, **92** (1988) 591.

III. Growth System for the Metalorganic Chemical Vapor Deposition of InN and InGaN Solid Solutions for Optical Semiconductor Device Applications

A. Introduction

InN and InGaN compounds have potential for applications in optical semiconductor devices. With band-gap energies of 1.9 and 3.4 eV for InN and GaN, respectively, devices can be made covering blue and blue-green light emission ranges. Work has been done in making blue LED devices using a double-heterostructure architecture, among others. Nakamura reports an output power of 125 μW and a quantum efficiency of 0.22% with a peak wavelength of 440 nm for their device [1]. Other works have reported film growth, although characterization of the films has been limited [2-4]. The main problem with growing the InGaN films has been the indium incorporation, due to the high equilibrium vapor pressure of nitrogen over InN, which is several orders of magnitude higher than either GaN or AlN. At low processing temperatures, epitaxial InGaN compounds have been grown successfully, although the film quality and optical properties have been poor. At higher processing temperatures film quality is good and optical properties improve, however, the incorporation efficiency of indium goes down as shown in Fig. 1. As a result, typical high temperature processing (>800°C) requires high ammonia flow rates and V/III ratios as large as 20,000 [2,3]. Compositional control in InGaN films has only been achieved for relatively low growth temperatures, up to 650°C [2].

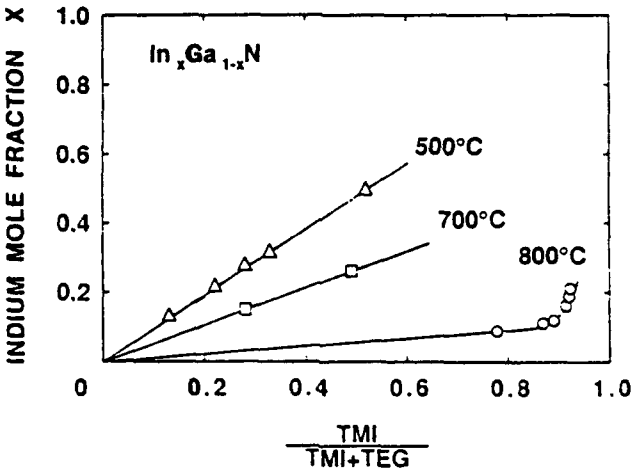

Figure 1. Relation between indium mole fraction of InGaN and the flow rate ratio of indium source to the sum of group III sources [3].

It has been shown that InN undergoes the following decomposition:

$$InN\ (s) \rightarrow In\ (l) + 1/2\ N_2\ (g).$$

Other work has show that decomposition starts as low as 550°C [5, 6]. As a result, it is easy to see why at higher temperatures the growth of InN films becomes difficult and why the indium incorporation in InGaN films decreases. As higher processing temperatures are required for better optical properties, a processing technique addressing the problems of the InN/InGaN system is needed. In this paper we introduce a chemical vapor deposition (CVD) system in which the crystal growth problems are addressed.

B. Experimental Procedure

Figure 2 shows a schematic of the CVD system we will use to grow the films. The design is a vertical cold wall reactor with metalorganic source gases. Using nitrogen as a carrier gas,

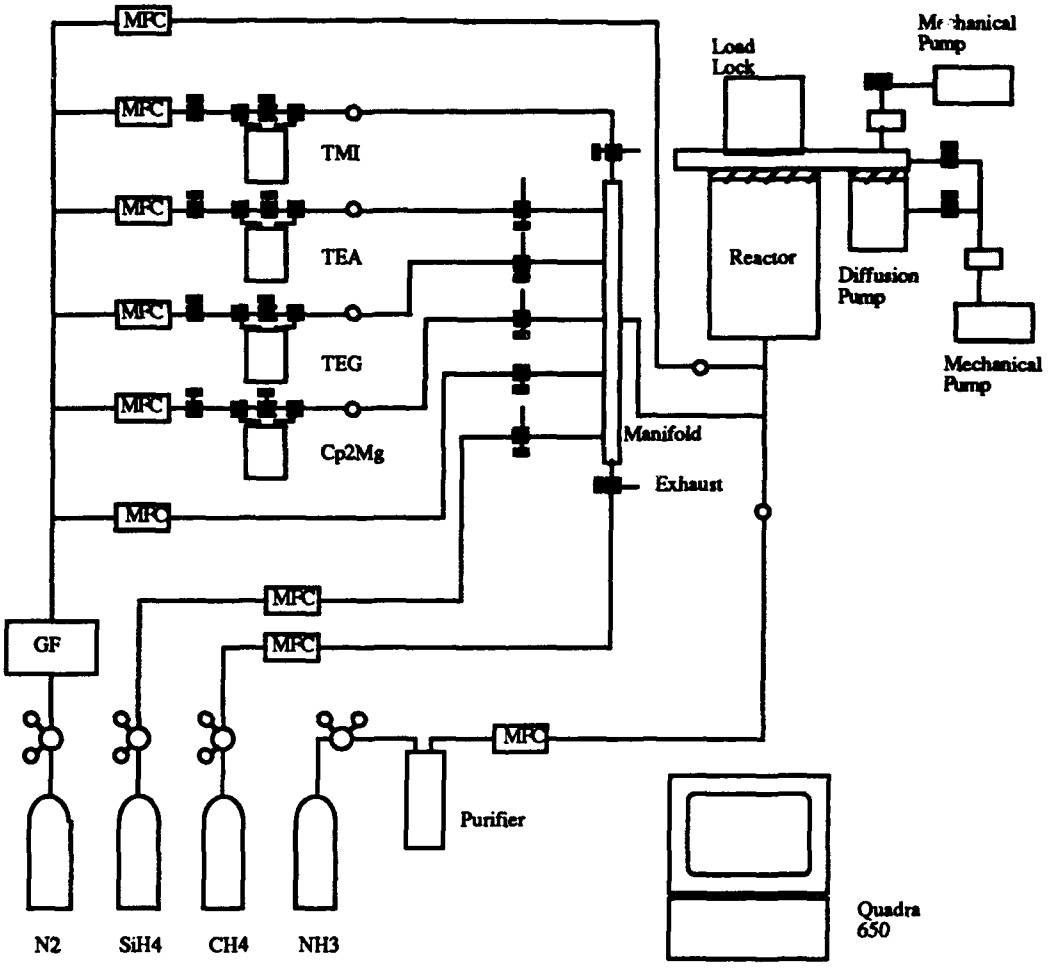

Figure 2. Schematic of chemical vapor deposition system.

the source gases and dopants enter a radial manifold where they mix and enter the reactor. Unlike conventional systems the source gases will enter at the bottom of the reactor and flow to the top. The source gases react with ammonia in the reactor on a resistance heated rotating substrate perpendicular to the flow direction. Excess nitrogen acts as a diluent in the reactor. The entire system will be computer controlled with an Apple Macintosh Quadra 650. This will allow for abrupt interfaces and good control in growing complex devices. InN and InGaN compounds will be grown on SiC substrates at various temperatures and compositions. As mentioned before, previous work has shown that high V/III ratios and large flow rates are required to grow quality films. In addition to varying the flow rates and ratios, the pressure of the system can be varied up to approximately 2500 torr. This will allow us to investigate the effects of processing pressure on the film quality.

A target composition for the nitride compound is $In_{0.2}Ga_{0.8}N$ which corresponds to an emittance wavelength of ~470 nm (bandgap of 2.64 eV), the wavelength used in blue LEDs for flat panel displays [3]. Figure 3 shows a representation of one of the device structures we will investigate in making an LED device. The structure is a p-GaN/n-InGaN/n-GaN double heterostructure LED. It will be grown on a SiC substrate with an AlN buffer layer. The n- and p-type dopants are Si and Mg, respectively. This and other devices will be investigated once film growth in the system has been characterized.

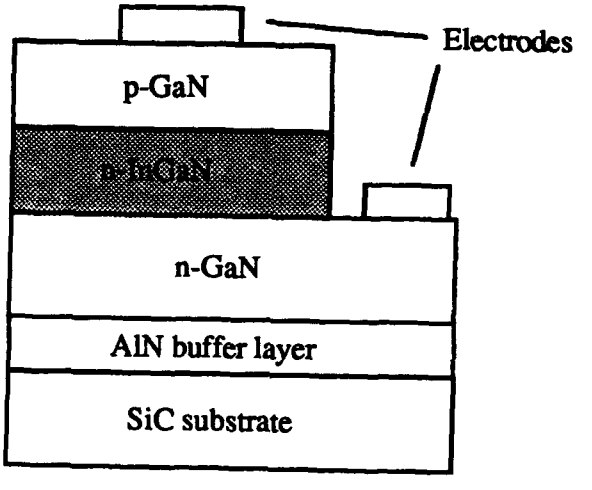

Figure 3. Structure of the DH blue LED (After [1]).

C. Discussion

The choice of reactor design comes from investigating the transport phenomena in the CVD process. The reactor geometry has considerable impact of the flow structure and by

appropriately designing the reactor it is possible to minimize the detrimental flow characteristics of vertical cold wall CVD systems. Examining several of the factors governing the transport phenomena in CVD we can see why the inverted geometry design lends itself to the InN/InGaN system.

Thermal Effects and Flow Patterns. Complex flow structures develop in CVD reactors due to large thermal gradients between the heated substrate and the cold walls. This leads to buoyancy-driven secondary flows superimposed on the forced flow of gases entering the reactor. Recirculation cells form above the suceptor in conventional flow reactors as result of these recirculations [7]. This effect can be controlled using high inlet flow rates, but there are limits to how close the inlet can be to the heated substrate without unwanted decomposition or predeposition in the inlet. However close the inlet is to the substrate, there will be a sudden increase in cross-sectional area as the gases enter the reactor, resulting in a decrease in linear flow velocity. This increases the potential for buoyancy-driven recirculation. Inverting the reactor so the buoyancy and inlet flow directions are aligned eliminates the major cause of thermal convections [8]. Radial temperature gradients may still drive flows, but with good temperature uniformity across the substrate this effect can be reduced. With an inverted geometry the flow from the gas inlet to the suceptor becomes controlled by the inlet flow rate which improves film thickness uniformity.

Suceptor Rotation. A rotating suceptor is often used in CVD systems to produce more uniform films. Rotation of the suceptor at high speeds emulates a rotating-disk flow which is advantageous in creating a uniform mass-transfer layer. As a result, the film thickness and growth rate are increased. The suceptor rotation also stabilizes the flow through the reactor by assisting the forced flow [7].

System Pressure. To obtain uniform deposition and abrupt interfaces CVD systems are often operated at reduced pressure with high flow rates. This is a result of the need to decrease the residence time of the reaction gases in the reactor. In conventional systems, residence time increases with increasing pressure as thermally driven convection flows increase [7]. With an inverted geometry the recirculation effect is virtually eliminated due to the alignment of the buoyancy and flow directions, allowing for the operation of the reactor at higher pressures without flow deterioration at higher pressures. This, combined with a rotating suceptor, should allow for forced flow conditions at higher pressures than conventional systems allow. This is especially pertinent in the InN system, where the equilibrium vapor pressure of nitrogen is high. Using a higher pressure of nitrogen in the system we should be able to better control the decomposition of the InN films at higher temperatures. We will be able to investigate the effect of an increased system pressure on the growth of single crystal InN films at higher temperatures without having to compensate for decreased flow stability.

Junctions/Interfaces. Abrupt junctions and interfaces are necessary in producing complex devices for optoelectronics applications. As mentioned above, good interfaces require abrupt changes in gas sources, which depends on the gas residence time in the reactor. With the inverted geometry, residence times can be decreased, even at increased pressures. Computer control will also give good timing precision.

D. Future Research Plans /Goals

Over the next six months we will order the equipment needed for the system and assemble it. Preliminary work will involve characterizing the growth of films in the system and achieving a level of reproducibility. A study we plan to perform is with a series of InN film growths at a set temperature over a range of pressures. Measuring the film properties and with use of a statistical analysis computer program, we should be able to find the effect of processing pressure on the film quality.

E. References

1. S. Nakamura, M. Senoh, T. Mukai, Jpn. J. Appl. Phys., **31** (1993) L8.
2. N. Yoshimoto, T. Matsuoka, T. Sasaki, A. Katsui, Appl. Phys. Lett., **59** (1991) 2251.
3. T. Matsuoka, N. Yoshimoto, T. Sasaki, A. Katsui, J. Elect. Matls., **21** (1992) 157.
4. T. Nagatomo, T. Kuboyama, H. Minamino, O. Omoto, Jpn. J. Appl. Phys., **28** (1989) L1334.
5. Q. Guo, O. Kato, J. Appl. Phys., **73** (1993) 7969.
6. R. Jones, K. Rose, J. Phys. Chem. Solids., **48** (1987) 587.
7. Jensen, K. *Microelectronics Processing: Chemical Engineering Aspects*; American Chemical Society, Washington, DC, 1989, p. 199.
8. Jensen, K., Einset, E. O., Fotiadis, D. I. *Annual Review of Fluid Mechanics*; Annual Reviews Inc., Palo Alto, CA, 1991, p. 197.

IV. Deposition of GaN PN Junctions and TEM Study of the Microstructure of AlN and GaN Films Deposited by Modified Gas Source Molecular Beam Epitaxy

A. Introduction

The research regarding GaN pn junction blue light emitting diodes (LEDs) has made significant progress [1–4]. To date, all of these devices were made by MOCVD. However, to achieve p-type character, the Mg-, or Zn-doped GaN films must undergo a post-growth treatment such as Low-Energy Electron-Beam Irradiation (LEEBI) or annealing at high temperatures in a nitrogen environment.

We have shown that using a modified gas source molecular beam epitaxy system (GSMBE), we were able to deposit p-type Mg-doped GaN films directly, i.e., without any post-growth treatment. In this report, additional further success regarding the deposition of GaN pn junctions by this technique will be described.

Also in this report, we will show microstructural analysis by transmission electron microscopy of our AlN and GaN films deposited under various different growth conditions.

B. Experimental Procedure

The deposition system employed in this research was a commercial Perkin-Elmer 430 MBE system. This system consists of three parts: a load lock (base pressure of 5×10^{-8} Torr), a transfer tube (base pressure of 1×10^{-10} Torr), which also was used for degassing the substrates, and the growth chamber (base pressure of 5×10^{-11} Torr). Knudson effusion cells with BN crucibles and Ta wire heaters were charged with 7N pure Ga, 6N pure Al, 6N pure Mg and 6N pure Si, respectively. Ultra-high purity N_2, further purified by a chemical purifier, was used as the sources gas. The N_2 was excited by an ECR plasma source, which was designed to fit inside the 2.25 inch diameter tube of the source flange cryoshroud. The details of the system can be found elsewhere [5].

The substrates were (0001) oriented α(6H)-SiC wafers obtained from Cree Research, Inc. Prior to loading into the chamber, the α-SiC substrates were cleaned by a standard degreasing and RCA cleaning procedure. All substrates were then mounted on a 3-inch molybdenum block and loaded into the system. After undergoing a degassing procedure (700°C for 30 minutes), the substrates were transferred into the deposition chamber. Finally RHEED was performed to examine the crystalline quality of the substrates.

C. Results

Deposition of GaN pn Junctions. Based on previous research results of the deposition of individual p-type, Mg-doped GaN and n-type, Si-doped GaN films, we have deposited the GaN pn junctions by a two-step and one-mask process.

We first deposit Si-doped GaN on the substrate. During this step, we initially expose the substrates to pure Al followed by exposure of this Al to the plasma activated nitrogen species in order to form an AlN layer. By this procedure, we have eliminated a thin amorphous layer on the substrate surface due to the plasma exposure. The film growth was subsequently started using the deposition conditions listed in Table I. An AlN buffer layer, having a thickness of about 150Å, was used to reduce the lattice mismatch and was followed by a layer of Si-doped GaN, which was ~3000Å thick.

Table I. Deposition Conditions for Si-doped GaN Films

Nitrogen pressure	2×10^{-4} Torr
Microwave power	50W
Gallium cell temperature	990°C
Aluminum cell temperature	1120°C
Silicon cell temperature	1180°C
substrate temperature	650°C
Al layer	2 monatomic layer
AlN buffer layer	150~200Å
Si-doped GaN	3000~4000Å

Then the sample was taken out of the system and a mask with defined open area was put on the top of the sample. With this mask we can make electrical contacts on the covered area of n-type Si-doped GaN, since we do not have a GaN etching facility to form the contacts.

Secondly, a layer of Mg-doped GaN (~3000Å thick) was deposited on the masked n-type GaN film by the conditions listed in Table II.

Characterization of GaN pn Junctions. Currently, we have only made IV measurements on these GaN pn junctions. The contacts for the measurement were made by two spring probes. IV curves were measured by a Hewlett Packard 4145 Semiconductor Parameter Analyzer. Typical IV curves are shown in Fig. 1 for the GaN pn junction on a sapphire substrate and in Fig. 2 for the GaN pn junction on an α-SiC substrate. The p-type character of the top Mg-doped GaN films was verified by the hot probe method.

Table II. Deposition Conditions for Mg-doped GaN Films

Nitrogen pressure	2×10^{-4} Torr
Microwave power	50W
Gallium cell temperature	990°C
Magnesium cell temperature	~300°C
substrate temperature	650°C
Mg-doped GaN	3000~4000Å

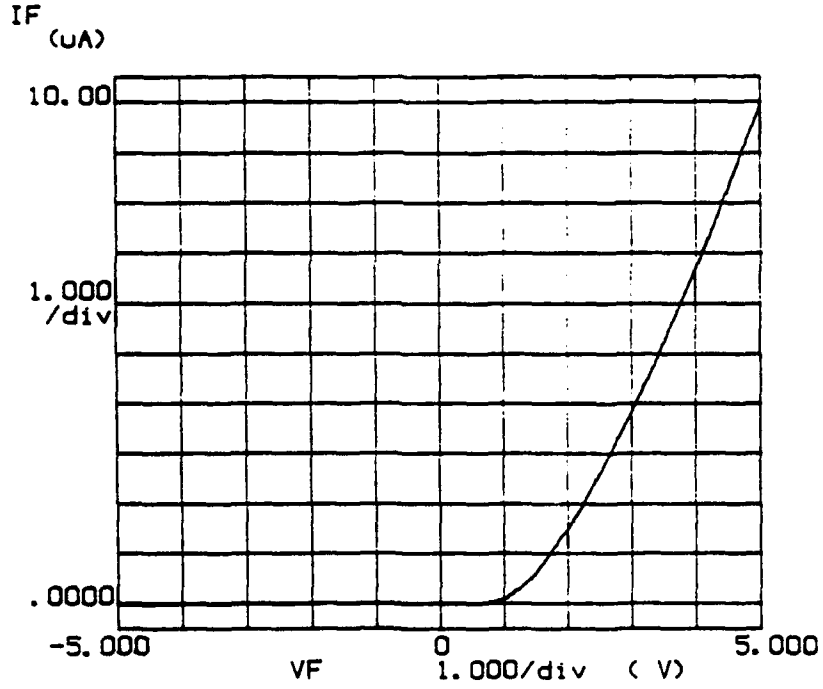

Figure 1. IV curve for the GaN pn junction on (0001) sapphire substrate.

Rectifying characteristics have been observed for the pn GaN junctions on both α-SiC and sapphire substrates. The turn-on voltages for both junctions are about 2 volts. At the same bias, the forward current for the junction on an α-SiC substrate is much larger than the junction on a sapphire substrate.

Further investigation of these junctions is underway, such as ohmic-metal contacts on either n- or p-type GaN layers, reactive ion etching of GaN films in order to deposit n- and p-type GaN layers without interruption, as well as electroluminescence measurements.

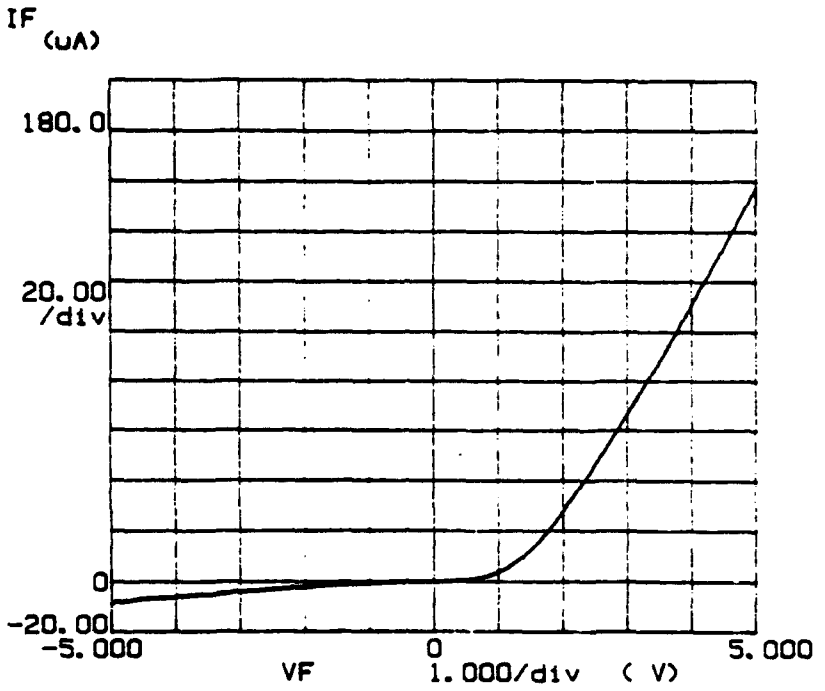

Figure 2. IV curve for the GaN pn junction on (0001) α-SiC substrate.

Electron Microscopy Characterization of AlN and GaN Films. The microstructure of the nitride films deposited by GSMBE was characterized by Transmission Electron Microscopy (TEM). The effect of various deposition conditions on the microstructure was investigated.

The TEM was performed in a JEOL 4000EX operated at 400kV. High resolution images were recorded using a 1mr convergence semi-angle at Scherzer defocus (~ –47nm). Cross-sectional transmission electron microscopy (XTEM) samples were prepared using standard techniques.

TEM Characterization of AlN Films. Previously, high quality AlN films had been deposited as buffer layers for the growth of GaN films using a modified GSMBE system. High resolution TEM indicated that these films had a highly oriented columnar structure [6]. Here we have investigated any structure change with respect to an increase in film thickness. As shown in Fig. 3, when the film thickness is increased above the critical thickness while maintaining the same deposition conditions, the density of defects which are parallel to the growth surface has greatly increased. The average width of the columnar features is about the same as that seen in the thin, ~100Å, AlN buffer layers. Both AlN films exhibited single crystal RHEED patterns.

The deposition temperature of our AlN films (~650°C) is much lower than what is most commonly used for MOCVD (above 1000°C). To improve the quality of the AlN films, the deposition temperature was raised to 1100°C while keeping other conditions the same. Figure 4

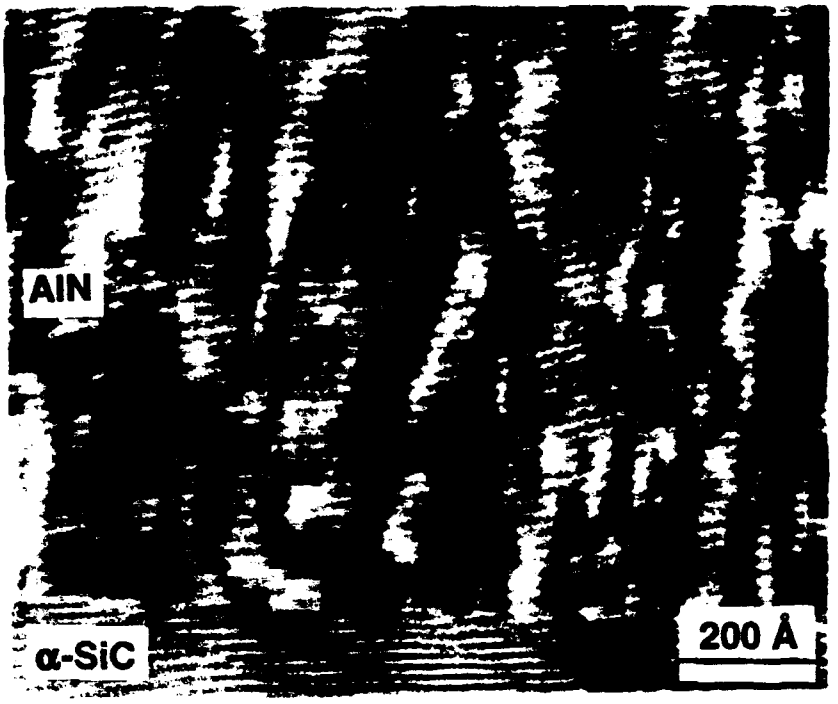

Figure 3. TEM micrograph of an AlN film deposited at 650°C.

is a TEM micrograph of an AlN film deposited at this higher temperature, 1100°C. Defects running perpendicular to the substrate have been greatly reduced, and defects parallel to the growth surface have been removed. A high resolution TEM micrograph of this AlN film, Fig. 5, shows the epitaxial AlN/α-SiC interface.

Figure 4. TEM micrograph of an AlN film deposited at 1100°C.

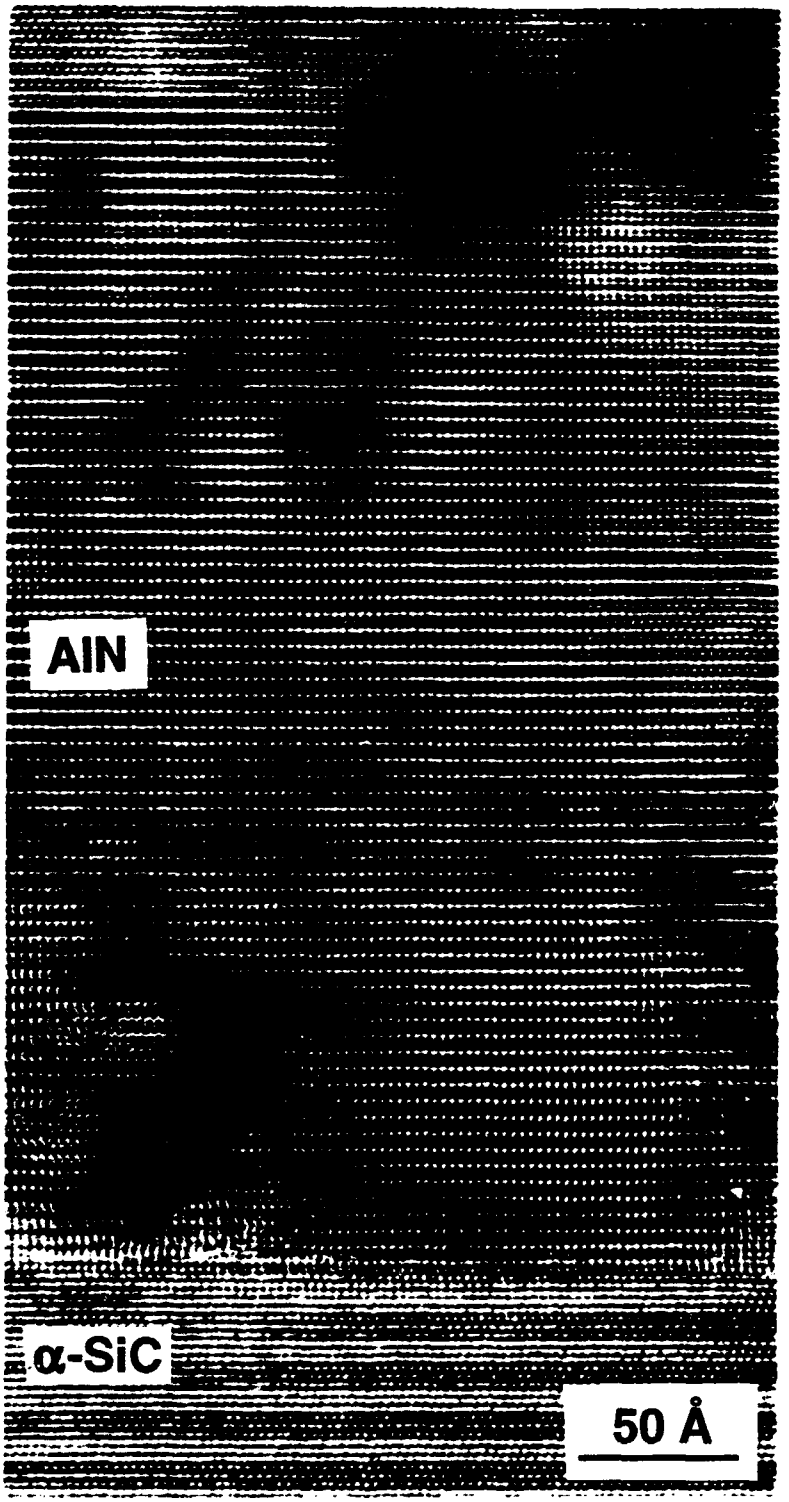

Figure 5. HRTEM micrograph of AlN film deposited at 1100°C.

TEM Studies of GaN Films. By a modified gas source molecular beam epitaxy system high quality GaN films have been deposited on both sapphire and α-SiC substrates [6]. RHEED, X-ray diffraction and electron diffraction have indicated that the films are single crystalline. However, as we reported before, TEM revealed that the GaN films still had a columnar

columnar structure. In order to reduce or eliminate these columnar features, we have investigated the effects of various different growth conditions. We limited our study to GaN films deposited on (0001) α-SiC substrates.

The TEM micrographs shown in Fig. 6 are of two GaN films deposited under the same growth conditions except for differing buffer layers. The film shown in Fig. 6 (a) has an AlN buffer layer for which the AlN was deposited at the same temperature as the GaN (650°C), while in Fig. 6 (b), there is no buffer layer. In the film with the buffer layer, there are fewer defects in the GaN close to the AlN buffer layer although increase in number further from the buffer layer. Comparison of Figs. 6 (a) and (b) reveals that the film without the buffer layer has more defects which are parallel to the growth surface and more of a columnar structure than the film with the buffer layer (with respect to the region of GaN close to the buffer layer). Since we know that the growth of high quality, epitaxial AlN films has been achieved at a higher deposition temperature on α-SiC substrates, we have attempted to eliminate the

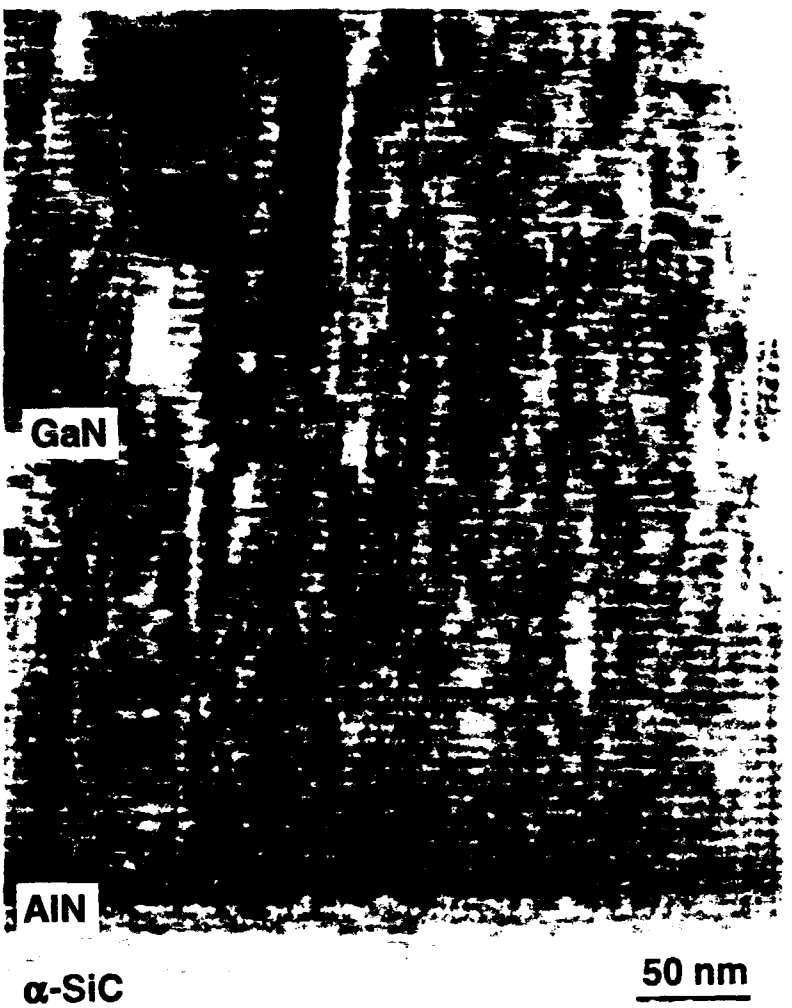

Figure 6. TEM micrograph of (a) GaN(650°C)/AlN(650°C)/α-SiC.

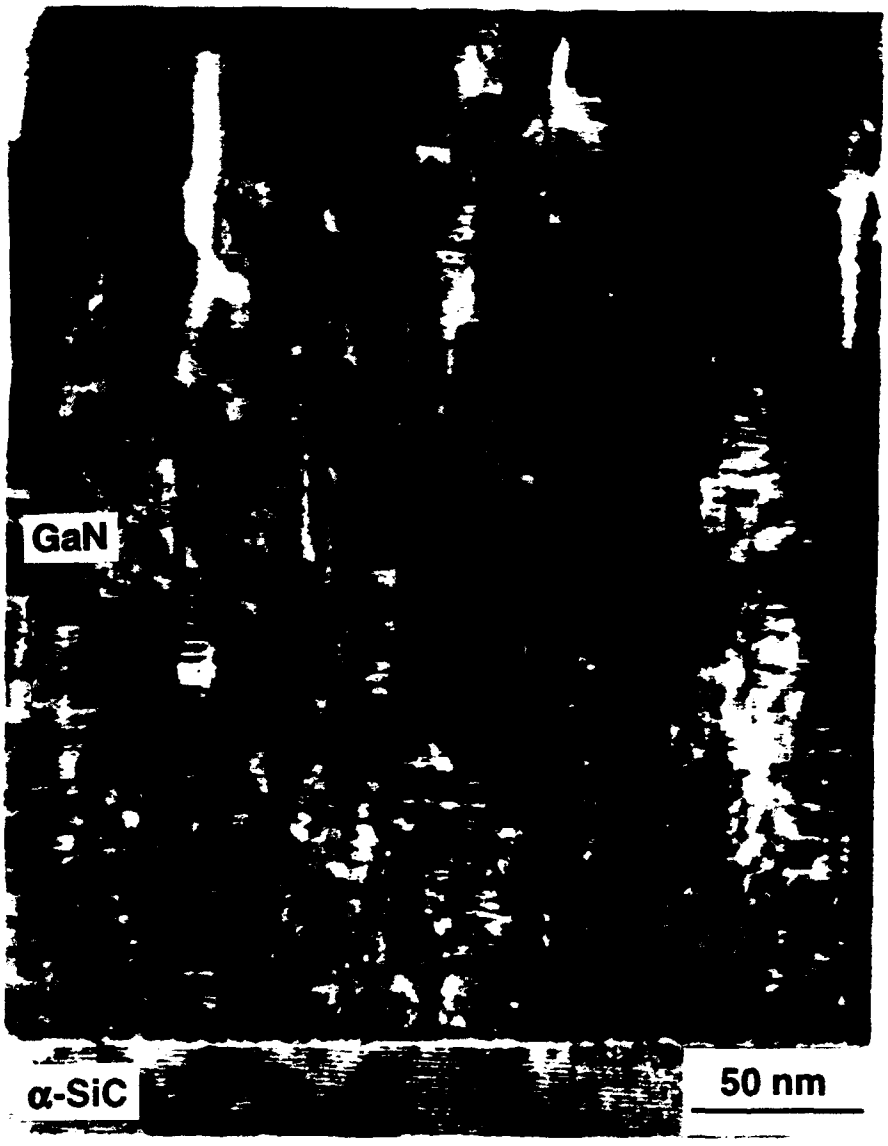

Figure 6. Continued—TEM micrograph of (b) GaN(650°C)/α-SiC.

columnar structure by depositing the AlN buffer layer at 1100°C proceeded by the deposition of GaN at 650°C on this AlN layer. Scanning electron microscopy showed very fine surface features, however, XTEM revealed that the film again consisted of a columnar structure, as shown in Fig. 7. No apparent improvement was gained from the increase in deposition temperature of the AlN layer.

Figure 8 is a TEM micrograph of a GaN film deposited at a reduced deposition rate (five times less) and longer deposition time than the GaN film shown in Fig. 7. Again there was no apparent improvement. Furthermore, the columnar features of the film in Fig. 8 increased in number as the growth proceeded. This is similar to what was observed in the film shown in Fig. 6(a).

Figure 7. TEM micrograph of GaN(650°C)/AlN(1100°C)/α-SiC.

D. Discussion

There have been a lot of reports recently on the deposition of high quality single crystal GaN films [2,4,7–9]. There are two key factors realized by most MOCVD research groups, that is: i) the need for low temperature deposition of AlN or GaN buffer layers with a thickness of about 300~500Å; ii) the thickness of the GaN films needs to be 3mm or more. To date, no clear microstructural images have been presented of these high quality single crystal GaN films, especially those revealing the change in film structure with the different film thicknesses. However, several TEM pictures of the buffer layer or GaN layer near the substrate interface have been reported [9,10]. In the above section, we have presented TEM results for our GaN films deposited at various growth conditions.

In summary, we have realized that, like MOCVD, the GaN films with the buffer layer are better than the GaN films without the buffer layer. It is has been generally accepted that the buffer layer is either for stress relief or for reduction of the lattice mismatch between the

Figure 8. TEM micrograph of GaN(650°C)/AlN(1100°C)/α-SiC, the deposition rate for the GaN film was five time less than the rate for the GaN film in Figure 6.

substrate and the GaN film; the lattice mismatch between AlN/α-SiC or AlN/sapphire is less than that between GaN/α-SiC or GaN/sapphire, respectively. However, even though AlN has been used as a buffer layer between GaN and the substrate, there is still a 2.4% lattice mismatch at the GaN/AlN interface. The columnar features we have observed in the GaN films may result from the lattice mismatch. As the GaN film becomes thicker, the stress due to lattice mismatch builds up, and the columnar features become more significant. This is quite different from what MOCVD results indicate. That is, single crystal GaN film growth can be accomplished only when the films were 3mm or more in thickness.

To obtain very high quality GaN films, the columnar structure must be eliminated throughout the films. The deposition temperatures of GaN by GSMBE were much lower than

what has been used in MOCVD. However, in the low pressure deposition process of GSMBE, the deposition temperature is really limited by the desorption rate of GaN [11]. As we have shown before, when the growth temperature was increased to 900°C almost no GaN film was deposited. Therefore, we have to pursue another way to overcome the columnar structures in the films if we cannot increase the deposition rate of the GaN films dramatically by GSMBE.

As we indicated before, the lattice mismatch still exists even when epitaxial AlN was used as a buffer layer between GaN and the α-SiC substrate. In contrast to MOCVD, in which the AlN buffer layer can be amorphous or polycrystalline, we cannot deposit epitaxial GaN films by GSMBE unless the AlN buffer layer is of good crystal quality. Therefore, the 2.4% lattice mismatch between AlN and GaN may play an important role in the columnar features in the GaN film. A direct way to reduce this lattice mismatch is to deposit an epitaxial buffer layer consisting of an AlN layer slowly graded to GaN on the substrate followed by the deposition of a GaN film on this graded buffer layer. However, as we found in our preliminary study, there was an abrupt change from an AlN-rich layer to a GaN-rich layer instead of a gradual graded layer. This is possibly due to the stronger attraction of Al to N than the attraction of Ga to N. Therefore, further research needs to be carried out to improve the deposition of a real graded layer.

F. Future Research Plans

As noted in the discussion part of this report, due to the limitation of GSMBE a graded $Al_xGa_{1-x}N$ solid solution buffer layer, from x=1 to x=0, would be an ideal solution for the homoepitaxy growth of GaN. Some of our future efforts will involve the growth of good quality graded $Al_xGa_{1-x}N$ solid solution buffer layers. The feasibility of designing an ammonia cracker cell to provide a source of atomic nitrogen is also being investigated. This source, if proved viable, will replace the ECR in the GSMBE system for growth of GaN. The ionized nitrogen species produced by the ECR may be causing damage to the GaN films, and if the species can be eliminated from the growth process, the GaN film growth can be further optimized. We will also continue our efforts to make GaN pn junction LED and other devices. Regarding the latter, the basic devices that would be the simplest to fabricate are a simple p-n junction and a Schottky diode. Cross sections of these devices are shown in Figs. 9 and 10, respectively. One difficulty in the fabrication of these devices will be the need to etch the nitride films in order to achieve a back side contact and device isolation (to produce the mesa structure as shown in Fig. 11) so the device can be electrically characterized. The etching of the films will be done in collaboration with K. Gruss and the nitride RIE etch facility (see later section).

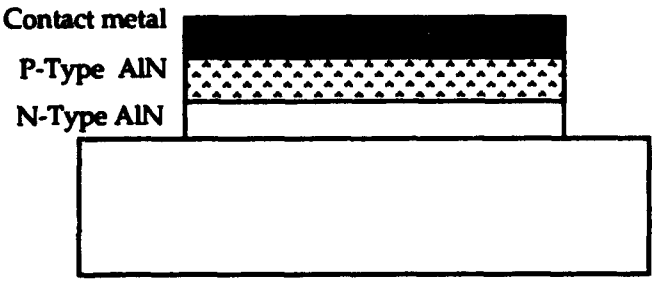

P-N Junction Mesa

Figure 9. P-N junction device.

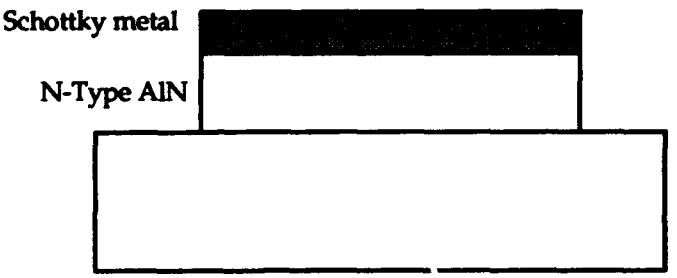

Schottky Diode Mesa

Figure 10. Schottky diode device.

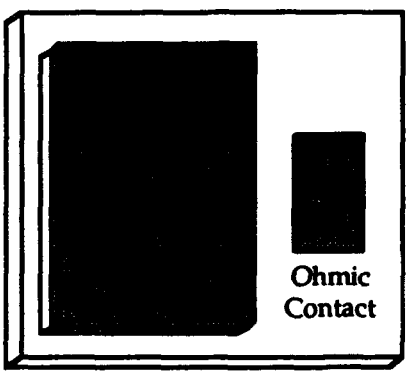

MESA Structure

Figure 11. Mesa structure for device isolation.

A MESFET device will also be fabricated to produce this device, two types of contacts will be deposited on the surface of the film using the pattern shown in Fig. 12. This will create a junction at the gate contact and thus make a transistor. These contacts will be

deposited directly onto the surface of the film and thus will require only photolithography to pattern the contacts.

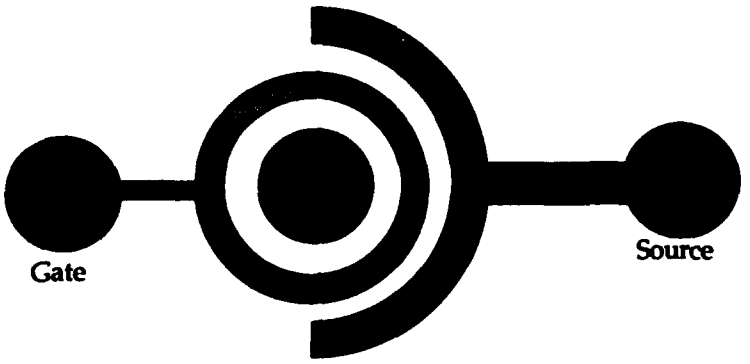

MESFET Structure

Figure 12. MESFET device contact pattern.

G. References

1. B. Goldenberg, J. D. Zook and R. J. Ulmer, Appl. Phys. Lett. **62**, 381 (1993).
2. I. Akasaki, H. Amano, N. Koide, M. Kotaki and K. Manabe, Physic B **185**, 428 (1993).
3. M. R. H. Khan, I. Akasaki, H. Amano, N. Okazaki and K. Manabe, Physic B **185**, 480 (1993).
4. S. Nakamura, M. Senoh and T. Mukai, Jpn J. Appl. Phys. **32**, L9 (1993).
5. Z. Sitar, M. J. Paisley, D. K. Smith and R. F. Davis, Rev. Sci. Instrum. **61**, 2407 (1990).
6. R. F. Davis *et al.*, R. F. Davis *et al.*, in Final Technical Report N00014-90-J-1427, P34–35 (1992).
7. M. A. Khan, J. N. Kuznia, D. T. Olson, R. Kaplan, J. Appl. Phys. **73**, 3108 (1993).
8. I. Akasaki, H. Amano, M. Sassa, H. Kato and K. Manabe, J. Crystal Growth **128**, 379 (1993).
9. J. N. Kuznia, M. A. Khan, D. T. Olson, R. Kaplan and J. Freitas, J. Appl. Phys. **73**, 4700 (1993).
10. N. Kuwano, T. Shraishi, A. Koga, K. Oki, K. Hiramatsu, H. Amano, K. Itoh and I, Akasaki, J. Crystal Growth **115**, 381 (1991).
11. N. Newman, J. Ross, and M. Rubin, Appl. Phys. Lett. **62**, 1242 (1993).

V. Development of a Photo- and Cathodoluminescence System for Optical Studies of III-V Nitride Films

A. Introduction

Luminescence is the emission of photons due to excited electrons in the conduction band decaying to their original energy levels in the valance band. The wavelength of the emitted light is directly related to the energy of the transition, by E=hv. Thus, the energy levels of a semiconductor, including radiative transitions between the conduction band, valance band, and exciton, donor, and acceptor levels, can be measured.[1,2]

In luminescence spectroscopy, various methods exist to excite the electrons, including photoluminescence (photon excitation), and cathodoluminescence (electron-beam excitation). In each technique, signal intensity is measured at specific wavelength intervals using a monochrometer and a detector. The intensity versus wavelength (or energy) plot can then be used to identify the characteristic energy band gap and exciton levels (intrinsic luminescence) of the semiconductor, and the defect energy levels (extrinsic luminescence) within the gap.[1]

Both photo- and cathodoluminescence analysis has been performed on AlN, GaN, and $Al_xGa_{1-x}N$ semiconductors.[3-15] Much of the work has been in measuring the low temperature GaN luminescence peaks. Work on AlN has been limited by the energy gap of 6.2 eV, which corresponds to a wavelength (200 nm) that is lower than most of the optical light sources. An excimer laser using the ArF line (193 nm) could possibly be used, although no one has attempted this to date. Caution must be taken when operating at these wavelengths.

Few time-resolved luminescence measurements have been performed on AlN and GaN. In a time-resolved measurement a pulsed source is used to excite the sample, and the luminescence is measured at short sampling intervals after the pulse. The result is an intensity vs. time plot. Time resolved spectroscopy is useful for separating the emission bands of the investigated samples with different decay times. It is often used to measure donor-acceptor recombination rates and minority carrier lifetimes.

Depth-resolved information can be obtained using cathodoluminescence, since generation depth varies with beam voltage. This technique is particularly useful for studying ion implanted semiconductors and layered structures.

B. Experimental Procedures

A combined photo- and cathodoluminescence system has been assembled and is currently being tested. A schematic view is shown in Fig. 1, and a block diagram is shown in Fig. 2. The sample is in a UHV chamber, and the monochrometer and collection optics are

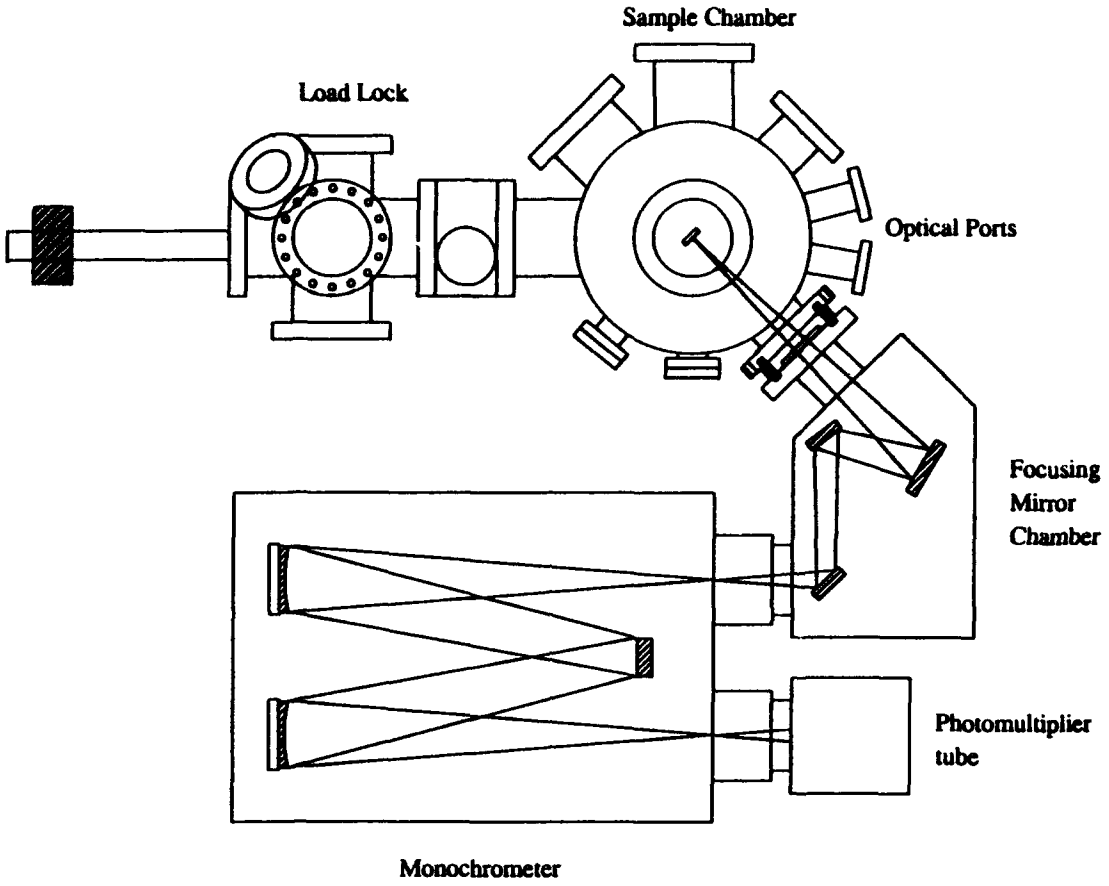

Figure 1. Schematic of the combined photo- and cathodoluminescence system.

in a vacuum environment. The sample is attached to a cryostat from APD cryogenics, which will allow for luminescence measurements at temperatures down to 4.2 K. The monochrometer is a McPherson model 219 vacuum monochrometer. Its focal length is .5 m, with a wavelength resolution of .04 nm at 313.1 nm. Two optical sources and a beam blanking electron gun will be used as the excitation sources. A Liconix He-Cd laser is currently being used; it is a continuous wavelength laser that operates at wavelengths of 325 nm, with a power of 15 mW. A pulsed excimer laser is the other optical source; it operates at wavelengths of 193 nm (6.4 eV), 248 nm (5.0 eV), and 308 nm (4.0 eV); and so it can be used to measure the luminescence of AlN.

A Kimball Physics electron gun is used for cathodoluminesence measurements. It has maximum beam voltage of 10 keV and a maximum beam current of 450 uA. By varying the beam voltage it will be possible to perform depth-resolved spectroscopy.

The beam blanking capability of the electron gun will make it possible to do time-delay studies of the semiconductors.

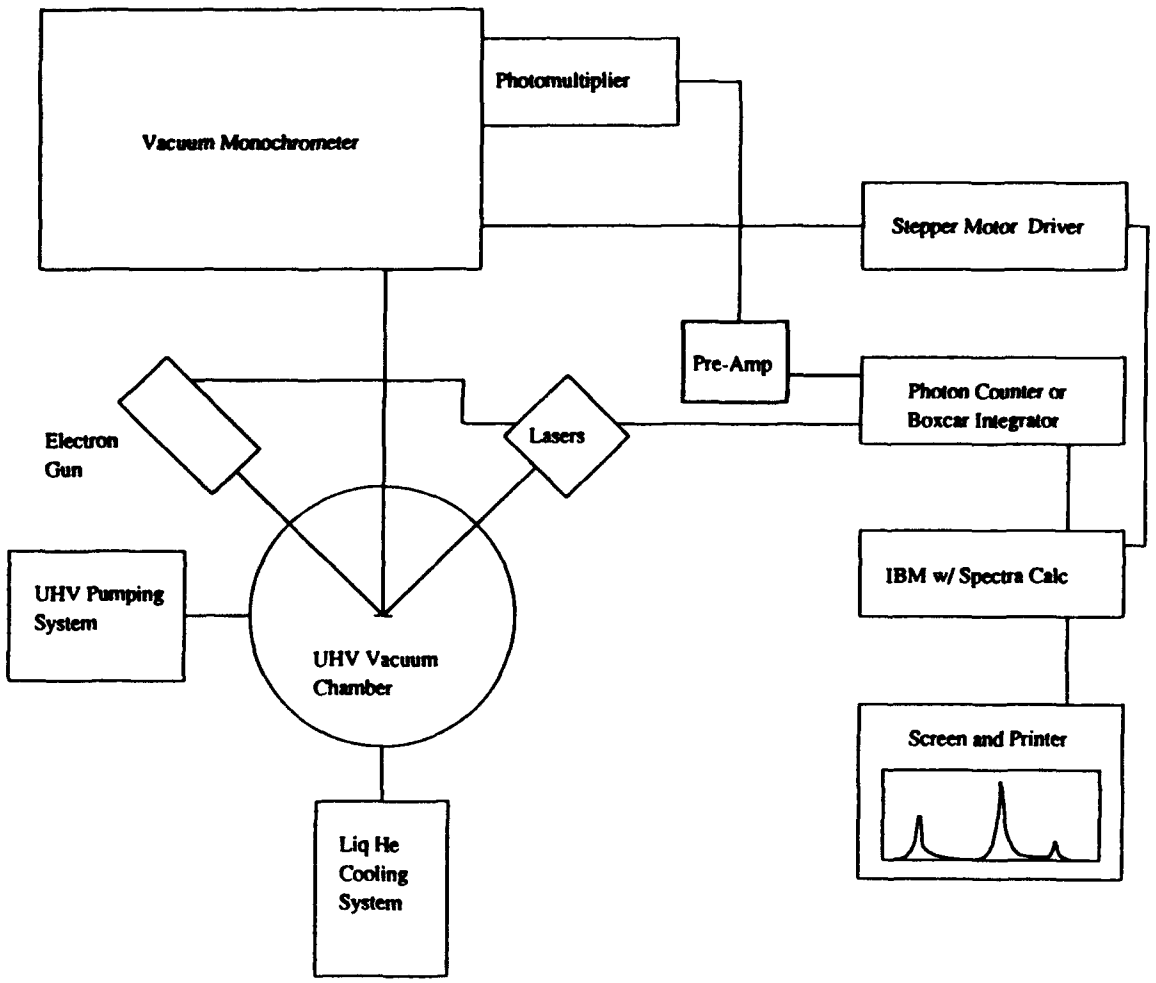

Figure 2. Block diagram of the combined photo- and cathodoluminescence system.

C. References

1. B. G. Yacobi and D. B. Holt, *Cathodoluminescence Microscopy of Inorganic Solids*, Plenum Press, New York (1990).
2. Micheal D. Lumb, Ed., *Luminescence Scpectroscopy*, Academic Press, New York (1978).
3. S. Strite and H. Morkoç, J. Vac. Sci. Technol. B, **10** (4) 1237-1266 (1992).
4. R. A. Youngman and J. H. Harris, J. Am. Ceram. Soc., **73** [11] 3238-46 (1990).
5. M. A. Kahn, R. A. Skogman, J. M. Van Hove, S. Krishnakutty, and R. M. Kolbas, Appl. Phys. Lett. **56** 9130 1257-59 (1990).
6. V. F. Veselov, A. V. Dobrynin, G. A. Naida, P. A. Pundur, E. A. Slotensietse, and E. B. Sokolov, Inorganic Materials, **25** (9) 1250-4 (1989).
7. J. N. Kuznia, M. A. Kahn, D. T. Olson, R. Haplan, and J. Freitas, J. Appl. Phys. **73** (9) 4700-4702 (1993).
8. M. R. H. Khan, N. Sawaki and I Akasaki, Semiconductor Science and Technology **7** 472-7 (1992).
9. K. Maier, J. Schneider, I. Akasaki, and H. Amano, Jpn. J. Appl. Phys., **32** (6) 846-848 (1993).
10. I. Akasaki, and H. Amano, J. Crystal Growth, **99** 375-80 (1990).
11. S. Yoshida, H. Okumura, S. Misawa, and E. Sakuma, Surf. Sci., **267** (7) 50-53 (1992).

VI. Contact Formation in GaN and AlN

A. Introduction

The formation of ohmic contacts with semiconductor materials and devices is a fundamental component of solid state device architecture. As device size has diminished and the scale of integration has increased, the quality of these interfaces has become an increasingly important concern. In addition, the presence of parasitic resistances and capacitances, such as those existing at contact interfaces, becomes more detrimental at higher operating powers and higher oscillation frequencies. The development of adequate and reliable ohmic contacts to the compound semiconductors, particularly those with wider band gaps, has met a number of challenges. The subject of ohmic contacts to p- and n-type III-V compounds, mostly GaAs, AlGaAs, and InP, has received a great deal of attention over the past decade, and significant advances have been made [1-12]. By comparison, the III-V nitrides have received little attention in this regard. However, interest in these materials has been renewed in recent years as thin film growth techniques have improved, p-type doping in GaN and AlGaN solid solutions has been achieved, and p-n junctions have been fabricated.

The majority of successful ohmic contact systems that have so far been implemented with the more conventional compound semiconductors have relied upon alloying (liquid-phase reaction) or sintering (solid-phase reaction) via post-deposition annealing treatments, and/or the presence of high carrier concentrations near the interface [1,2,6,12]. However, many otherwise successful ohmic contact systems have only limited thermal stability and are subject to degradation—usually in the form of extensive interdiffusion, interfacial reaction, and interphase growth, accompanied by increase in contact resistivity—under subsequent thermal processing steps. It is reasonable to suppose that the cleanliness and preparation of the semiconductor surface prior to contact deposition plays a significant role in the behavior of the interface, and there are indications in the recent literature that support this [2,11-13]. Thorough oxide removal is especially important, though it may well prove to be a persistent challenge with Al-containing compounds in particular.

In this study, two main approaches are being taken in the development of ohmic contacts to GaN and AlN. The first approach is similar to that which has resulted in the majority of successful ohmic contacts to the more conventional compound semiconductors such as GaAs: the creation of high carrier concentrations in the semiconductor at the metal interface by means of alloying, sintering, or implantation of dopant species. The so-called pinning of the Fermi level at this surface, particularly with GaAs, results in a more or less fixed potential barrier at the metal interface. In the case of the pinned Fermi level of GaAs, the approach has generally been to shrink the width of the depletion layer by means of increasing the carrier concentration to the point where carrier tunneling through the barrier occurs readily. Even

with optimization of contact composition and annealing times and temperatures, the lowest contact resistivities (ρ_c) have been obtained only on the most heavily doped materials. Though there are indications that high doping levels and extensive interfacial reactions through alloying and sintering are not essential for ohmic contact formation in all cases, these processes have proven useful for minimizing ρ_c [2,11-13].

The other approach toward ohmic contact formation to be taken in this study involves the Schottky-Mott-Bardeen (SMB) model of semiconductor interfaces [14,15]. In this model the relative values of work function of the materials involved determine the band structure of the interface and thus the nature of any potential barriers present. The presence of interfacial states at the semiconductor surface can interfere with the alignment of the Fermi level across the interface and overshadow the effect of the inherent difference in work function between the two materials. The III-V nitride compounds are more ionically bonded than their phosphide and arsenide counterparts, as a result of larger electronegativity differences between the component elements. According to the observations of Kurtin *et al.* [16], this fact indicates that the nitrides should experience less Fermi level stabilization or "pinning" at the surface than do the more covalent compounds. Thus, the barrier heights of contacts to the nitrides should be more dependent on the contact material than is the case with the more conventional and more covalent semiconductors such as Si, GaAs, InP, SiC, etc. With the work of Foresi and Moustakas [17,18], this concept is beginning to be investigated. The SMB model also indicates that the cleanliness of the interface plays an important role in its electrical behavior, particularly in the minimization or elimination of any insulating layers at the interface.

To date, several alloyed and sintered contact strategies, having demonstrated effectiveness with GaAs—and, in the case of Au, with GaN—have been undertaken with GaN and AlN. The tighter bonding of Ga and Al to N, in comparison to As, suggests that higher temperatures and possibly longer times are required for interfacial reactions to take place, and that some reactions may be inhibited or prevented. The behavior of the systems examined so far has been consistent with these suppositions. Contact strategies derived from GaAs technology will continue to be characterized in this study, and an investigation of the roles of work function differences and interfacial cleanliness will be undertaken in the coming weeks.

B. Experimental Procedure

Film Deposition. Doped GaN and AlN films for contact studies were grown on 6H-SiC substrate crystals by means of ECR plasma enhanced molecular beam epitaxy (MBE). Magnesium was grown into the films as the p-type dopant and Ge was used to grow n-type materials, as described in other sections of this report.

Four different contact systems were deposited and examined during this reporting period: single Au layers, Zn/Au, Cr/Au, and AuGe/Ni/Au. The single Au layers were 2500Å thick; the Zn/Au and Cr/Au structures consisted of 350Å layers of Zn or Cr followed by 2300Å of gold. The alloyed AuGe contact consisted of successively deposited layers of AuGe 88:12 eutectic alloy (m.p. 360°C) (1500Å), Ni (420Å), and Au (3000Å). Contact metals were deposited by means of electron beam evaporation using a Thermionics evaporation system having a 3 kW 5-source electron gun. The 5-source capacity of the e⁻-beam hearth allowed the deposition of multiple layers of different metals without breaking vacuum to change sources. Prior to metals deposition, the nitride films were cleaned with a 50:50 $HCl:H_2O$ dip and rinsed in DI water. A shadow mask was used during deposition to create rectangular-bar TLM (transmission line model) patterns for contact resistivity (ρ_c) measurements, as described in the preceding semiannual report of June 1993. Film thicknesses were monitored using a quartz crystal oscillator.

Contact characterization. After deposition, I-V measurements were taken between separate pads of the TLM patterns, using tungsten probe tips and an HP 4145C Semiconductor Parameter Analyzer. Annealing treatments were performed in a flowing N_2 atmosphere at successively higher temperatures using a Heatpulse 410 rapid thermal annealing (RTA) furnace. Once the contacts began to show distinctly linear I-V behavior after sufficient annealing, TLM measurements were taken by measuring the total resistance between identical contact pads as a function of separation distance l. The contact resistivity was obtained from the plot of R(l) vs. l, as described by Reeves and Harrison [19]. The simplifications inherent in this model yield values for ρ_c that represent an upper limit; thus, the measured values are conservative assessments of performance.

C. Results

Au contacts on Mg:GaN. Gold contacts deposited on p-GaN were rectifying as-deposited. Though the as-deposited contacts were rectifying, neither were they close to being ideal Schottky contacts; reverse bias leakage was significant and there was not a clearly linear region in the log I-V plot from which an ideality factor could be calculated. Subsequent annealing steps eventually resulted in linear (ohmic) I-V behavior once sufficiently high temperatures were reached. Figure 1 shows an I-V plot for the p-GaN/Au contact as-deposited (a) and annealed at 800°C for 5 minutes (b). Noticeably linear behavior in the low voltage region was first detected after annealing to 650°C; further annealing at higher temperatures reduced the ρ_c measurable by TLM. At 700°C the ρ_c was 3130 $\Omega \cdot cm^2$; after annealing at 800°C for 10 minutes the ρ_c was reduced to 54 $\Omega \cdot cm^2$.

After annealing at 750°C the appearance of the Au contact surface changed; what was originally a shiny, mirrorlike Au surface became somewhat dull to the eye, suggesting

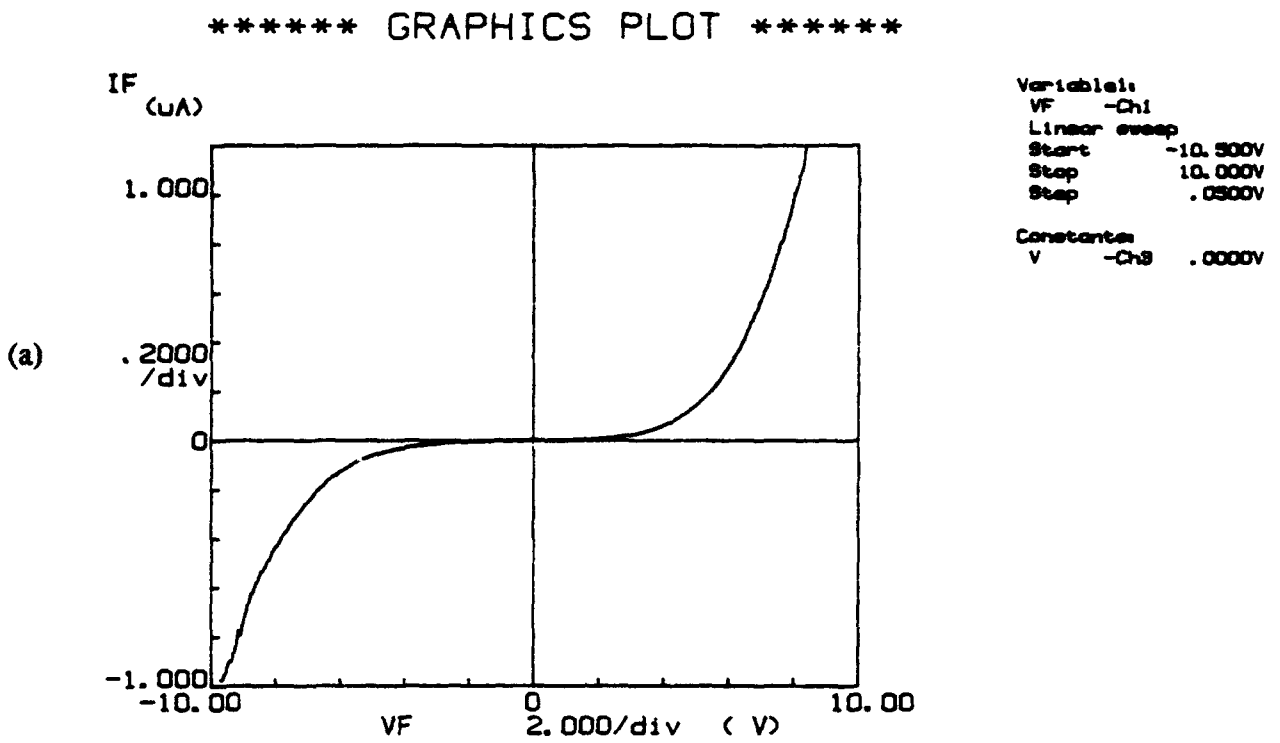

(a)

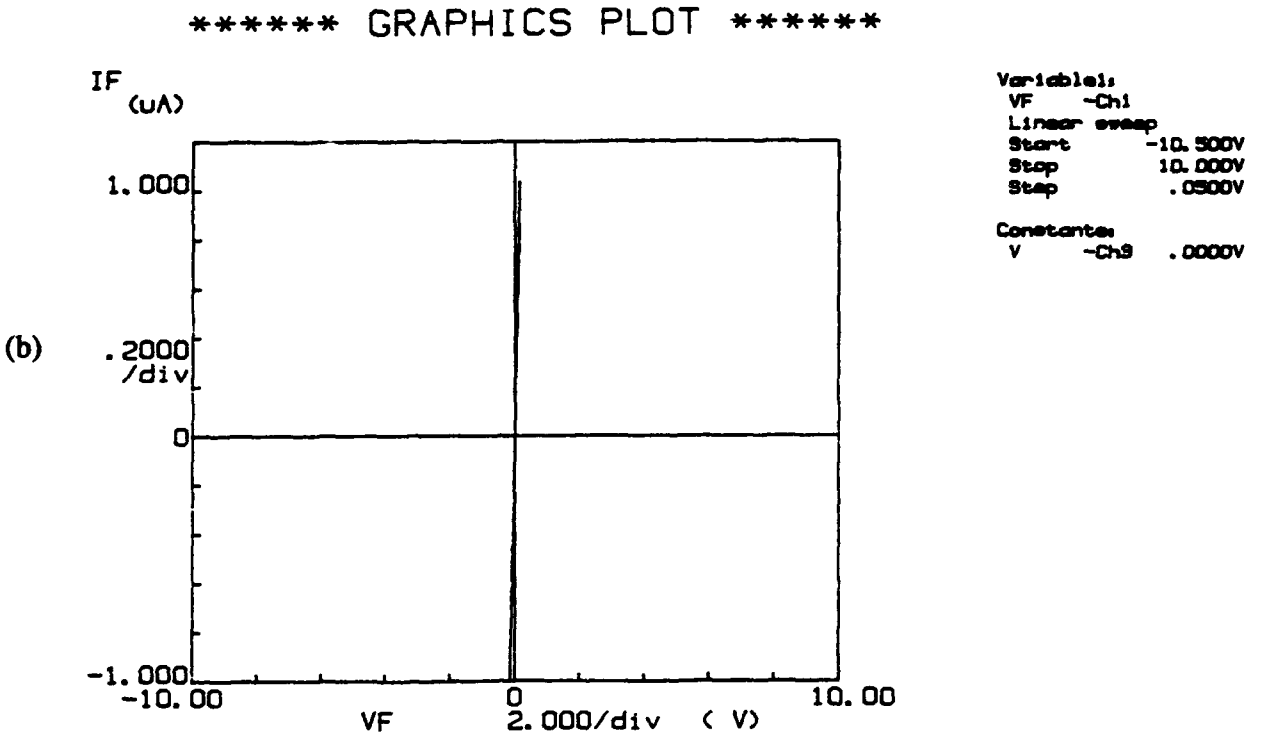

(b)

Figure 1. I-V data for Au contacts on Mg-doped GaN: (a) as-deposited (b) annealed to 800°C for 5 min.

increased roughness. This change in appearance progressed with time upon heating at higher temperatures. An SEM image of the corner of an as-deposited Au contact pad is shown in Figure 2(a). The as-deposited Au surface was similar in texture to the underlying GaN surface. Some shadowing effect from the contact mask was revealed, and this effect was taken into account in the pad spacing for the TLM measurements. After annealing at 800°C for 10 minutes, large lumps developed in the metal film along with tiny specks on the surface. Holes >1 μm in size opened up in the Au film, and the metal at the shadowed edge had "balled up" on the GaN surface. At higher magnification, the evidently bare GaN surface could be seen through the holes in the Au layer.

Zn/Au and Cr/Au contacts on Mg:GaN. Though chemically different, the Zn/Au and Cr/Au contacts on Mg-doped GaN behaved similarly in many respects. Initially both contacts showed linear I-V behavior in the low-voltage region in the as-deposited state, but in both cases the slope of the I-V trace was so shallow, i.e. the resistance was so high, that reliable contact resistivity values could not be obtained. Figure 3 shows examples of I-V traces of Zn/Au contacts in the as-deposited condition and after annealing at 650°C. Over the wider voltage range of ±10 V the I-V plots of the Cr/Au contact consistently showed more curvature, but in the range ±2 V the behavior of both samples was similar. After annealing at 650° both contact systems had become sufficiently conductive for taking TLM measurements, which yielded ρ_c values of 3180 Ω·cm² for Cr/Au and 11850 Ω·cm² for Zn/Au.

The appearance of the Au surface of the Cr/Au contacts changed after annealing at 450°C for 2 minutes. The previously smooth mirror-like surface appeared to roughen on a fine scale, similar to the Au-only contacts described above but slightly lighter in color. Microscopic examination of the surface after annealing at 650°C for 3 minutes, shown in Figure 4, revealed many small pores, shallow crevices, and lumpiness on a very fine scale. The shallow, crater-like depressions in the lower part of the image were left by the probe tips during electrical measurements. The appearance of the Zn/Au contacts remained shiny throughout.

AuGe/Ni/Au contacts on Ge:AlN. The AuGe/Ni/Au contacts deposited on Ge:AlN exhibited significant changes as a result of annealing. This contact system was rectifying in the as-deposited condition, but developed linear I-V behavior in the low-voltage region upon annealing. However, annealing through 650°C did not sufficiently reduce the contact resistance enough for reliable TLM measurements. The I-V behavior varied somewhat over different areas of the AlN surface; the I-V plots shown in Figure 5 represent a middle ground of measured behavior that ranged from being more rectifying and more asymmetric that those shown to being more ohmic-like and more symmetrical.

(a)

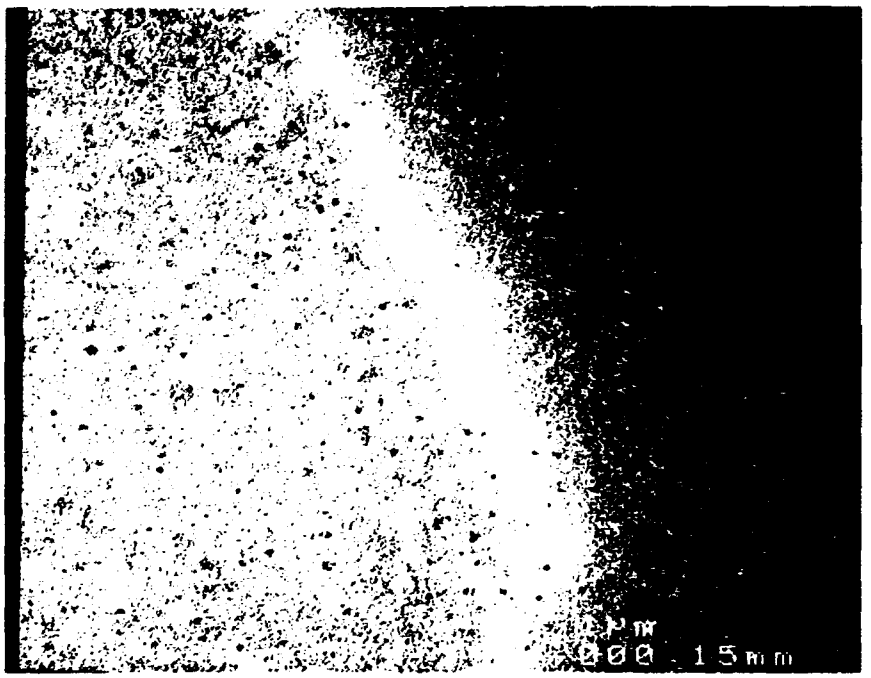

(b)

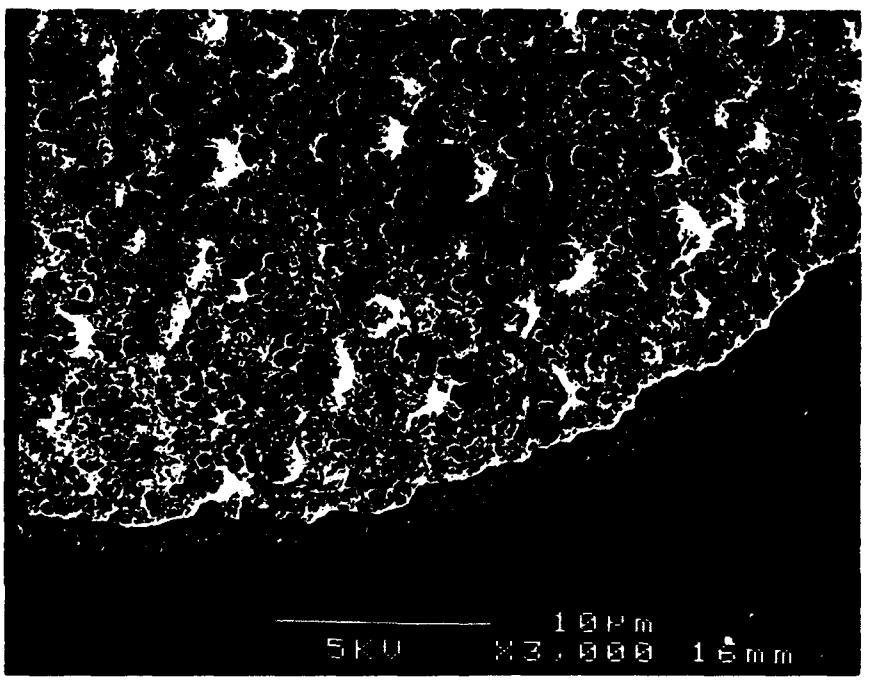

Figure 2. Edge of Au contact pad on Mg:GaN: (a) as-deposited (b) annealed at 800°C for 10 minutes.

(a)

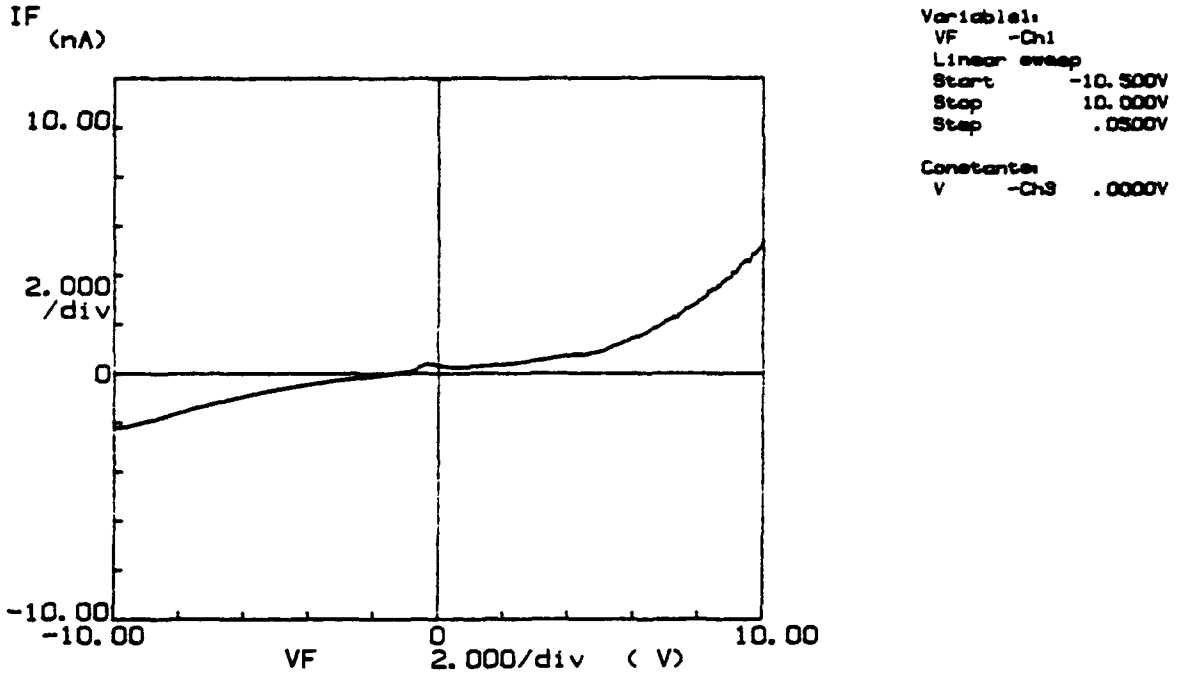

(b)

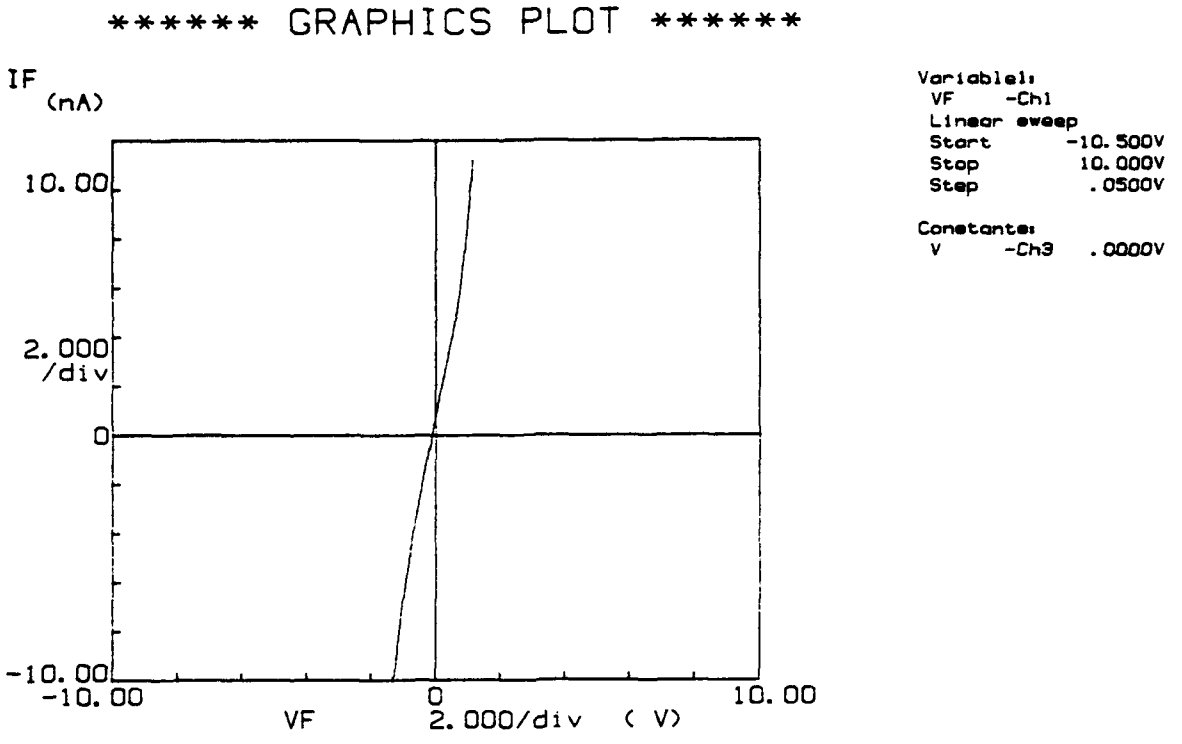

Figure 3. I-V data for Zn/Au contacts on Mg-doped GaN: (a) as-deposited (b) annealed to 650°C for 3 minutes. Data for Cr/Au contacts were similar.

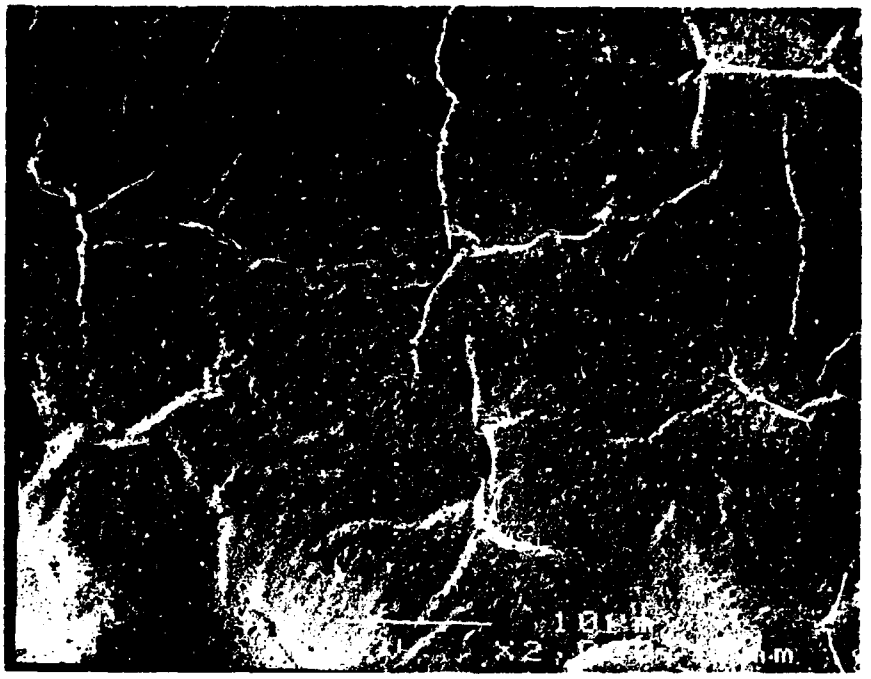

Figure 4. Surface of Cr/Au contact pad on Mg:GaN, annealed at 650°C for 3 minutes.

Under the microscope, this contact system revealed yet a different texture than the others. The edge of a AuGe/Ni/Au pad annealed at 650°C for 3 minutes is shown in Figure 6. Like the Au-only film, the metal at the shadowed edge balled up, but to a lesser degree than did Au. The contact surface itself appears to have a fine polycrystalline texture of mixed orientation.

D. Discussion

Au contacts on Mg:AlN. The rectifying nature of the as-deposited Au contacts on undoped n-GaN was observed by Foresi and Moustakas in their contacts investigation [17,18]. However, the GaN material used by Foresi *et al.* was different than that used in this study; theirs was undoped and inherently n-type, indicative of a high background carrier concentration and defect density. According to the Schottky model, Au should form an ohmic contact on p-type GaN and a rectifying contact on n-type material. However, it should be pointed out that the exact value for the work function and/or electron affinity of GaN and their dependence upon doping levels have not been reproducibly and precisely established as yet. Foresi and Moustakas obtained ohmic contacts with Au on undoped n-GaN after annealing at 575°C for 10 minutes in a reducing atmosphere; according to their TLM measurements they achieved contact resistivities in the range $1.6\text{-}3.1\times10^{-3}\ \Omega\cdot cm^2$.

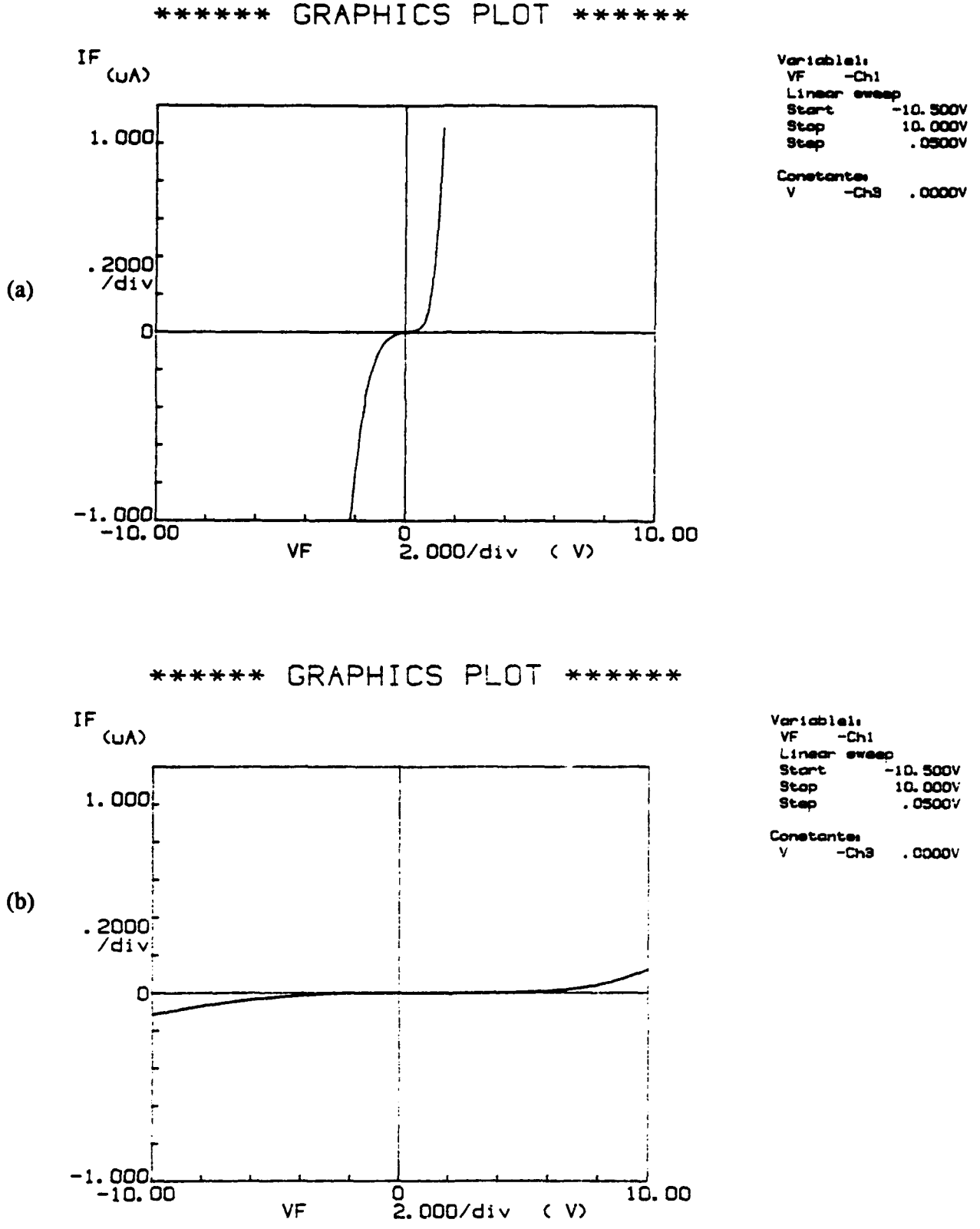

Figure 5. I-V data for AuGe/Ni/Au contacts on Ge-doped AlN: (a) as-deposited (b) annealed at 650°C for 3 minutes.

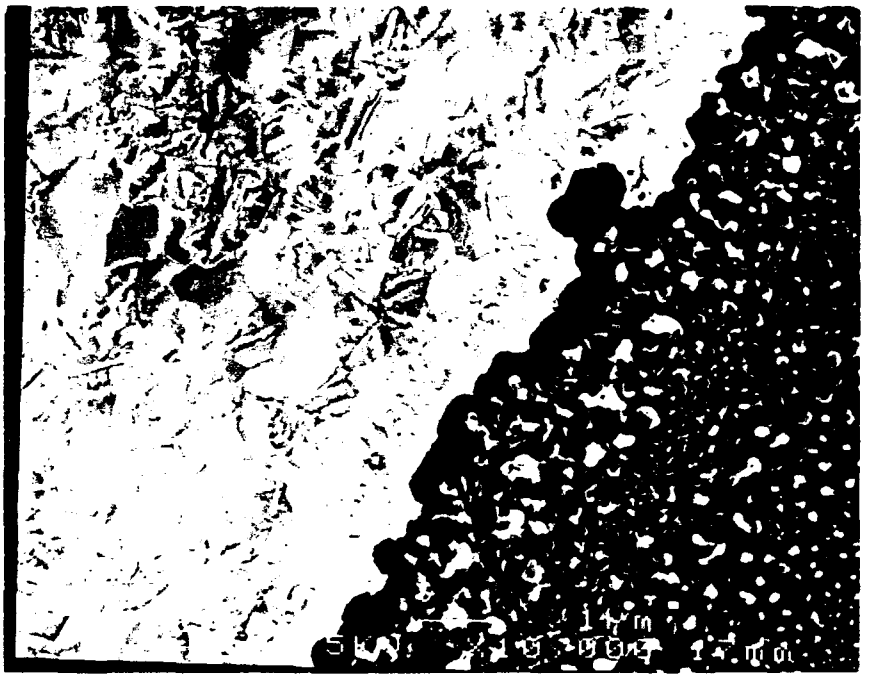

Figure 6. Edge of AuGe/Ni/Au contact pad on Ge:AlN, annealed at 650°C for 3 minutes.

In the present study, the contact resistivities obtained from Au on Mg-doped GaN were higher. The samples were annealed for short periods of time in an RTA furnace under flowing N_2. The purpose of performing the annealing under N_2 at atmospheric pressure for short times was to reduce the likelihood of generating N vacancies which are believed to be shallow donors that contribute to the background carrier concentration. While increasing the background carrier concentration may contribute to greater current transport in the semiconductor and across the contact interface and apparently reduce the ρ_c, in general such behavior would be detrimental to overall electronic properties and device performance. More extensive characterization of the electronic properties of our nitride films is needed to better correlate and understand the relationship between dopant concentration, carrier concentration and mobility, Fermi levels, and contact behavior. Improvements in our measurement capabilities, in terms of both equipment and sample preparation techniques, are underway.

The change in appearance and texture of the Au surface after high-temperature annealing is likely due to reactions and/or interdiffusion taking place between the Au and GaN. The lumpiness of the annealed Au film is indicative of metallurgical reaction and phase formation, and the balling-up effect implies a lack of good "wetting" of the GaN surface. Surface characterization and depth profiling by means of Auger electron spectroscopy (AES) will be performed shortly to determine the nature of any chemical changes that took place during annealing. Characterization by means of cross-sectional TEM (X-TEM) will also be

performed to investigate the interfacial structure in detail. A possible scenario is that under sufficient thermal activation Ga diffuses out of the GaN and into the Au layer and reacts to form compounds. Interfacial reactions with contacts on GaAs typically show a significant amount of interphase formation and roughening of the interface. The roughening of the interface due to reaction and phase formation may help to lower ρ_c by increasing the area of contact between the metal layer(s) and the semiconductor. Gallium nitride lacks the very mobile As sp cies and has stronger interatomic bonding, but sufficiently high temperatures can and favorable chemistry nevertheless free the Ga and N from one another. Depth profiling and cross-sectional examination will allow further clarification of these issues.

Zn/Au and Cr/Au contacts on Mg:GaN. The Zn/Au contact system has been used on p-GaAs with some success, but the exact mechanism of its behavior is not yet well understood [2,12]. As Zn acts as an acceptor occupying the Ga site, the Zn is thought to form a highly doped interfacial layer which allows carrier tunneling through the contact interface. Zinc and Cr have approximately similar work functions (ϕ_{Zn}= 4.33 eV; ϕ_{Cr}= 4.5 eV) and thus, according to the Schottky model, would both be rectifying on a p-type semiconductor having a lower work function (ϕ_{GaN} estimated to be 4.1 eV). Chromium is not used as an acceptor impurity in III-V compounds, but it is capable of assuming a variety of oxidation states between -2 and +6. As indicated on binary phase diagrams, both Zn and Cr have the capability of forming compounds with both Ga and Au, so the potential for interfacial reaction exists given sufficient thermal activation. It is possible that even if a pure contact metal does not have a favorable work function relationship to a semiconductor for ohmic contact formation according to the Schottky model, some of the interfacial compounds that may form could be more favorable. The changes in the Cr/Au contact top surface as a result of thermal treatment suggest interfacial reaction, though whether involving the Cr and Au only or the GaN as well is not clear as yet. The samples will receive further thermal treatment, and upcoming depth profiling and cross-sectional characterization will help determine what has taken place.

AuGe/Ni/Au contacts on Ge:AlN. This contact system has become a standard low-$_c$ contact for n-GaAs and the complex nature of its interfacial alloying reactions has received a great deal of study [2,11,12]. Its primary drawback is its relatively poor thermal stability when used with GaAs. After the initial alloying anneal, the electrical properties of AuGe contacts tend to change and degrade significantly upon exposure to subsequent thermal processing steps even at relatively low temperatures (below 500°C). As described above, it is expected that the much stronger interatomic bonding of GaN and AlN in comparison to GaAs will significantly increase the temperatures required for reactions and/or interdiffusion to take place. The other layered contacts, Zn/Au and Cr/Au, have been used with success on p-GaAs,

though the structure and properties of the interfaces have not been as thoroughly studied as has AuGe.

It is evident from SEM examination that the contact system experienced structural changes as a result of annealing treatment. There is no lumpiness as in the other roughened contacts, but rather a fine grain structure that was not apparent in the as-deposited state. However, the degree of interaction between the different layers cannot be determined from the surface texture. As with the other contact systems, further characterization will help to understand the annealed structure of this contact.

This first attempt at ohmic contact formation on doped AlN resulted in a very high contact resistivities. It is likely that the higher interfacial resistance and spatial inhomogeneity of these contacts were largely due to the presence of an insulating oxide layer on the AlN surface. Like the GaN surfaces, the AlN samples were cleaned with a standard HCl dip prior to metal evaporation. However, while HCl removes much of the Ga oxides from GaAs and GaN, it does not remove much of the more stable Al oxides and hydroxides. Since Al oxides have highly negative energies of formation and are very stable compounds, removing them from AlN will likely prove to be a challenge, as has been the experience with AlAs. If the oxide layers can be chemically stabilized and kept very thin, it is possible that the presence of a small amount of oxide can be relatively innocuous in terms of device performance. Atomic cleaning techniques under vacuum, such as plasma or ion etching, prior to contact deposition, are likely to result in substantial improvements of interface properties if structural damage to the semiconductor can be kept to a minimum. In situations where the contact metal can be deposited directly on top of the freshly-grown nitride film without breaking vacuum, such as in MBE growth, oxide formation would be avoided.

E. Conclusions

The work conducted in this study so far has shown that it is possible to form metal contacts with ohmic-like linear I-V behavior to doped GaN and AlN films. As yet these contacts exhibit high contact resistivities, but it is reasonable to expect that refinement of contact metals choice, surface cleanliness, and deposition procedures will result in substantial improvements. In the contact systems studied to date, there are indications that interfacial reactions took place during annealing that correlated with the development of linear I-V behavior and reductions in ρ_c. Further characterization of these contacts, particularly with AES depth profiling and X-TEM analysis, is needed to understand the chemical and structural changes that took place in the contacts as a result of thermal treatment.

F. Future Plans/Goals

In addition to chemical and structural characterization of the contact systems described in

this report, the next stage of this study is to investigate more carefully the effects of surface cleaning procedures and to produce more pristine interfaces for electrical characterization. Contacts will be deposited in a UHV e⁻-beam evaporation chamber that has a lower base pressure than the chamber used during this period and has an ion gun to use for surface cleaning as well as metal nitride film formation. Titanium nitride as an ohmic contact candidate for n-type nitride semiconductors was described in the preceding semiannual report, and will be investigated along with the more conventional metal systems.

G. References

1. T. C. Shen, G. B. Gao, H. Morkoç, J. Vac. Sci. Technol. B **10**(5), 2113 (1992).
2. R. Williams, *Modern GaAs Processing Techniques* (Artech House, Norwood, MA, 1990)
3. M. Murakami, Materials Science Reports (5), 273 (1990).
4. A. Piotrowska and E. Kaminska, Thin Solid Films **193/194**, 511 (1990).
5. A. Piotrowska, A. Guivarc'h and G. Pelous, Solid-St. Electron. **26**(3), 179 (1983).
6. V. L. Rideout, Solid-St. Electron. **18**, 541 (1975).
7. K. Tanahashi, H. J. Takata, A. Otsuki and M. Murakami, J. Appl. Phys. **72**(9), 4183 (1992).
8. H. J. Takata, K. Tanahashi, A. Otsuki, H. Inui and M. Murakami, J. Appl. Phys. **72**(9), 4191 (1992).
9. M. C.Hugon, B. Agius, F. Varniere, M. Froment and F. Pillier, J. Appl. Phys. **72**(8), 3570 (1992).
10. W. O. Barnard, G. Myburg and F. D. Auret, Appl. Phys. Lett. **61**(16), 1933 (1992).
11. G. Stareev, Appl. Phys. Lett. **62**(22), 2801 (1993).
12. E. D. Marshall and M. Murakami, in *Contacts to Semiconductors*, edited by L. J. Brillson (Noyes, Park Ridge NJ, 1993).
13. F. W. Ragay, M. R. Leys and J. H. Wolter, Appl. Phys. Lett. **63**(9), 1234 (1993).
14. H. K. Henisch, *Semiconductor Contacts*. (Clarendon Press, Oxford, 1984).
15. E. H. Rhoderick, *Metal-Semiconductor Contacts* (Oxford University Press, New York, 1988).
16. S. Kurtin, T. C. McGill and C. A. Mead, Phys. Rev. Lett. **22**(26), 1433 (1969).
17. J. S. Foresi, *Ohmic Contacts and Schottky Barriers on GaN*, M.S. Thesis, Boston University (1992).
18. J. S. Foresi and T. D. Moustakas, Appl. Phys. Lett. **62**(22), 2859 (1993).
19. G. K. Reeves and H. B. Harrison, IEEE Electron Device Lett. **EDL-3** 111 (1982).

VII. Reactive Ion Etching of GaN and AlN

A. Introduction

Semiconductor devices are the principle components of electronic and telecommunications systems [1]. In order to densely pack these microscopic components, unidirectional, or anisotropic, etching techniques are required to produce a fine network of lines. Wet etching processes found in many semiconductor manufacturing steps produce a multi-directional, or isotropically, etched material. This is undesirable for microcircuitry since the goal is to produce the smallest devices possible. Therefore, plasma-assisted processes, such as reactive ion etching (RIE), combine the physical characteristics of sputtering with the chemical activity of reactive species to produce a highly directional feature. RIE has the added advantage of providing a more uniform etch and a higher degree of material etch selectivity.

RIE has been employed to etch a wide variety of semiconductor materials including silicon-based materials [2-11], metals, like aluminum [3, 12-18] and III-V compounds, such as GaAs and InP [19-21]. However, plasma-assisted etching of newer III-V compounds, such as GaN and AlN, has been attempted by few investigators [20-24]. There has been wide spread interest in using these nitrides for semiconductor device applications requiring visible light emission, high temperature operation and high electron velocities [20]. Since these materials possess wide bandgaps and optical emissions spectra in the blue to near ultraviolet range, they are prime candidates for ultraviolet detection devices.

The objectives of this report are to discuss recent progress made in the field of reactive ion etching of gallium and aluminum nitride. In the following sections, a brief review of pertinent literature on plasma-assisted etching of gallium and aluminum compounds is provided along with a brief description of the reactive ion etching system and process gases.

B. Literature Review

Reactive Ion Etching of GaN. Since GaN is a direct transition material with a bandgap ranging from 3.4-6.2 eV at room temperature, it is an ideal candidate for the fabrication of shortwave length light emitters [20, 25]. High quality GaN films have been successfully grown by MOVPE [25], ECR-MBE [26, 27], MOCVD [28] and a layer-by-layer process [29] on a number of substrate. In order to fabricate complete device structures, reliable etching processes need to be developed. Since GaN is nearly inert to most wet etching solutions, with the exception of highly concentrated hot NaOH and H_2SO_4 [30], RIE may prove to be an effective method for the production of fine line patterning in semiconductor materials.

There have been a few reports of etching GaN by plasma-assisted processes [20-24]. Foresi [21] investigated fabrication techniques for ohmic contact and Schottky barriers on

GaN. One of the highlights of his work was the successful etching of GaN on sapphire substrate in Freon 12 (CCl_2F_2) and in hydrogen atmospheres operating at about 10 mTorr and 40 and 60 W of RF power. Results from SEM photographs showed that in the CCl_2F_2 plasma, GaN had been completely removed from areas that were not covered by photoresist, and that the sapphire substrate was nearly unetched. Foresi was able to obtain an etch rate of approximately 140 Å/min in the CCl_2F_2 plasma at 60 W, while the hydrogen plasma produced insignificant etching results. Etch selectivity between the GaN and photoresist was found to be 3:1. In another investigation, conducted by Tanaka et al. [20], reactive fast atom beam etching was employed to etch GaN on sapphire in a Cl_2 plasma at substrate temperatures ranging between 80-150°C. Etch rates of 1000-1200 Å/min produced relatively smooth surfaces and a well defined pattern of elongated rectangular bars on the sapphire substrate. More recently, S.J. Pearton et al. [22] have produced smooth, anisotropically etched GaN and AlN in low pressure ECR discharges of BCl_3/Ar, CCl_2F_2/Ar and CH_4/H_2/Ar. The etch rates of these nitrides were highly dependent on the DC bias voltage and ranges of 25-175 Å/min and 0-100 Å/min were reported for GaN and AlN, respectively. It is noted that hydrogen was added to the chlorine plasmas to facilitate removal of hydrogen from the surfaces of the nitride samples, thus producing smoother features. Also, Adesida *et al.* [23] employed reactive ion etching to produce 4000 Å thick lines in GaN with $SiCl_4$ plasmas. They found that the etch rate was independent of pressure but increased with self bias voltage. They obtained slightly overcut features with fairly smooth sidewalls at etch rates up to 500 Å/min. Experimental etching was also conducted with $SiCl_4$/Ar and $SiCl_4/SiF_4$, but the addition of Ar and F atoms to the plasma had no effect on the etch rate. In addition, residual Si and Cl were found on the GaN surfaces after etching.

Reactive Ion Etching of AlN. Aluminum nitride is a candidate material for optoelectronic devices because it possess a high electrical resistivity, high thermal conductivity, low dielectric constant and has a direct transition bandgap of 6.3 eV [31]. AlN films have been grown by several techniques including CVD, MBE and ALE, and on a variety of substrate materials including sapphire, silicon, spinel, silicon carbide and quartz [32]. Etching fine features in the AlN films is an important step in the fabrication of such devices. Though, only one report of etching of AlN is available in the open literature at this time [22], much work has been conducted on etching of metallic aluminum thin films [3, 12-18]. As a result, analogies to well established data for etching of aluminum are made. Although aluminum and AlN are very different materials, the chemistry and reactions in the plasma may be similar. So, it is proposed that reactive ion etching may also be an effective means for the application of fine line patterning of AlN.

A review of the literature shows that there are two primary methods employed for etching aluminum. Bruce and Malafsky [12] employed a parallel plate configuration (RIE) to

investigate the effects of Cl_2 on aluminum. They found that two processes are involved, namely, the removal of the oxide layer and etching the metal below it. For those experiments, it was hypothesized that BCl_3 gas was necessary for the removal of the oxide layer because it was responsible for the initiation of a reduction reaction with the oxide. In the RIE etching configuration, aluminum etched with a chlorinated gas is a purely chemical reaction with little contribution from ion bombardment. This conclusion was made as a result of the insensitivity of RF power to the etch rate [12]. Therefore, anisotropic etching was thought to have been the result of a sidewall passivation mechanism whereby a protective layer is formed on the vertical walls of the trench by reaction of H_2O or carbon containing species with the aluminum. Since ion bombardment is normal to the surface, the walls remained unetched. This mechanism was produced by the addition of $CHCl_3$ to the mixture of gases. Feature widths of 2.25 μm were produced by a gas mixture of Cl_2, BCl_3, $CHCl_3$ and He at about 1.2 mTorr. Helium gas was added to the mixture to reduce the amount of erosion of the photoresist.

The combination of an isotropic flux of reactive species with a highly directional beam of energetic ions, so called ion beam assisted etching (IBAE), has been employed for the anisotropic etching of aluminum by many investigators [13-15, 18]. For IBAE, the aluminum oxide layer can be physical removed by sputtering with Ar^+ or Xe^+ ions, whereas with RIE the oxide is removed chemically [13]. However, etching takes place again by chemical reaction of Cl_2 with the aluminum as determined by the lack of dependence of the etch rate on the ion energy and current [14, 15]. From a mechanistic point of view, Cl_2 adsorbs onto and diffuses into the aluminum resulting in the formation of aluminum chlorides. Al_2Cl_6 is the dominant etch product at lower temperatures (33°C), while $AlCl_3$ was observed at higher temperatures (210°C) [15]. Saturation of the etched surface with chlorine atoms occurs prior to desorption of $AlCl_3$.

The etch rate is dependent upon several parameters including the presence of residual gases in the chamber, substrate temperature, Cl_2 flux, ion beam and the presence of carbon containing species. Impurity gases in the chamber (i.e. H_2O, O_2, N_2, etc.) can react with the aluminum films and impede the etching process by leaving a residue on the etched surface. This reduces the amount of Cl_2 available for reaction and consequently lowers the etch rate [13]. The substrate temperature is another parameter that affects the etch rate of aluminum. Efremow et al. [13] observed a two-fold increase in the etch rate by heating the substrate from 0° to 100°C. It was hypothesized that the increase in temperature led to a higher evaporation rate of the product $AlCl_3$. In addition, they found that an increase in the Cl_2 flux produced a significant amount of undercutting due to the nondirectional flow of the Cl_2 gas. A higher degree of anisotropy was achieved by the combination of ion beam and Cl_2 flux. Efremow *et al.* suggested that sidewall passivation (by reaction of H_2O with the aluminum)

was partly responsible for the production of the very fine features in their samples. Submicrostructures of 80 nm wide lines were etched into a 100 nm thick aluminum film with 0.3 mTorr Cl_2 gas and 0.1 mA, 1 keV Ar^+ beam. Lastly, Park et al. [14] found that chemisorption of the halocarbon gas molecules, such as CCl_4 and CBr_4, onto the aluminum surface formed halogentated aluminum species along with an aluminum carbide. Therefore, a significant reduction in the etch rate was observed due to the difficulty encountered in removing the carbide from the surface.

C. Proposed Research

Experimental Apparatus. A schematic of the RIE system is shown in Fig. 1. The main components of the system include gas handling/storage, etcher, gas scrubber and mass spectrometer. Since toxic gases, such as BCl_3 and Cl_2, may be used to etch GaN and AlN, the system is designed for safe shutdown in the event of a power or water failure and/or inadvertent shutdown of the exhaust systems in the building.

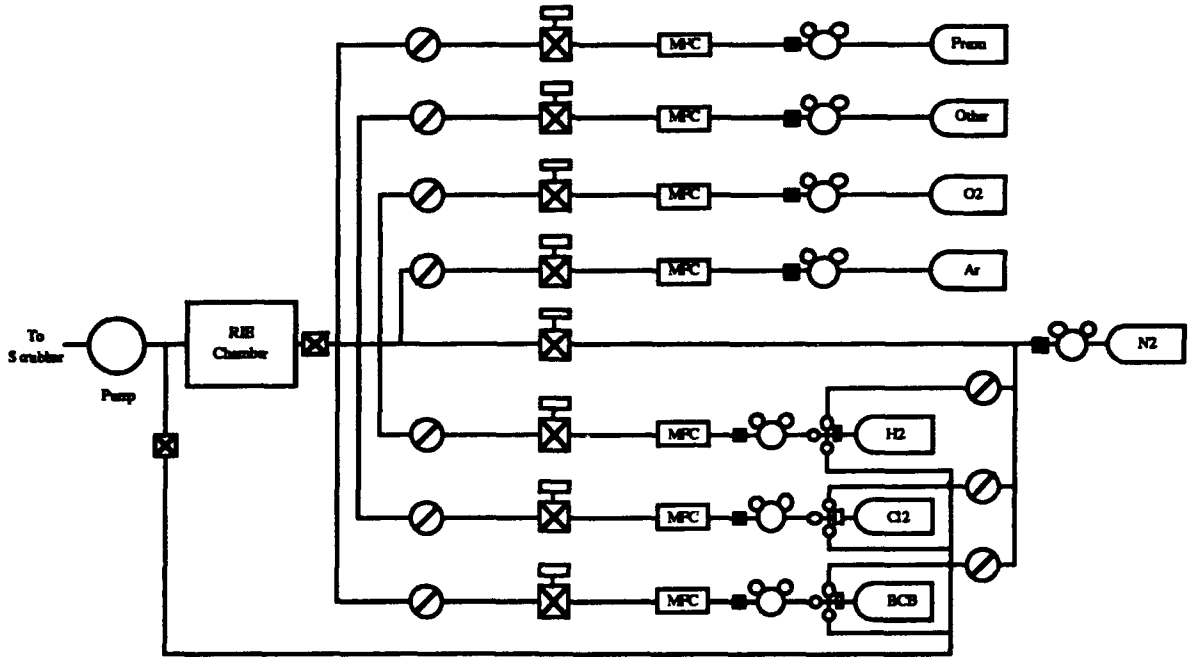

Figure 1. Reactive ion etching system.

The gas handling/storage sub-system consists of the gas storage cabinet(s), gas bottles, bottle regulators and necessary valves and tubing. Dry nitrogen will be used to purge the gas lines before and after every run to remove moisture and chlorine from the lines, thus reducing

the probability of corrosion of the gas lines. Mass flow controllers will be employed for accurate control of the process gases. In addition, pneumatic valves will be installed as a safety precaution. In the event of a power failure, interruption of the water supply or shutdown of the exhaust system, the solenoid actuated pneumatic valves will isolate the gas lines from the etch chamber.

The design of the etcher is based on that of the standard parallel-plate diode configuration in which the bottom electrode is powered by a RF power supply (see for example Ref. vanRoosmalen, 1984 #10). The etcher, a Technics 85 series RIE, consists of an anodized aluminum chamber with an anodized aluminum water-cooled, driven lower electrode. A 350 Watt, 13.56 MHz RF generator with auto impedance matching network produces the power required to maintain a glow discharge in the chamber. Safety interlocks are supplied by Technics to disable the power when the system is vented or a panel is removed. The chamber pressure is measured by a corrosion-resistant capacitance manometer (absolute pressure) which is mounted to the underside of the chamber. The two channels of process gas (made from stainless steel tubing) are isolated from the injection manifold by means of air-operated electrically actuated isolation valves. In addition, an 11 CFM two-stage corrosive-series direct drive rotary vane pump is supplied with the etcher.

Residual process gases and reaction by-products from the etcher will pass through a wet scrubber which is equipped with water inlet and water recirculation lines. These lines are monitored for water flow and exhaust ventilation and are an intregral part of the control system. Interruption of the water flow or inadequate ventilation will trip the pneumatic valves and close the gas lines. In addition, the pH level of the scrubber water will be tested and monitored prior to waste disposal.

Lastly, a mass spectrometer may be employed in the future for the detection and characterization of chemical species produced by the etching processes. It could also be used as a kind of end-point detection device. It is further hoped that this analytical instrumentation could provide necessary information for the determination of the success of the etching processes and could provide a basis for an understanding of the etching mechanisms.

Choice of Process Gases. There are a number of process gases that can be used to produce anisotropically etched features. For GaN and AlN, fluorine plasmas are impractical because involitile fluorides are formed with Ga and Al at the surfaces, therefore limiting desorption of reaction species from the surface [33]. Chlorine plasmas, on the other hand, have been used extensively for etching these compounds, see Section B above.

In etching GaN, the gases used by Tanaka [20], Foresi [21] and S. J. Pearton *et al.* [22, 24], namely CCl_2F_2, Cl_2 and BCl_3, will be employed first since those investigators reported successful results. Experimentation with other combinations of gases, such as iodine- and/or bromine-containing gas mixtures) is likely in order to obtain smooth, anisotropic features

with reasonably high etch rates. As for AlN, chlorine containing gases with additions of O_2, carbon containing gases and or noble gases (i.e. Ar, He, etc.) are likely candidate gases. Though, somewhat of a trial and error methodology will be followed until success is achieved. It is noted that for RIE, sidewall passivation may be an important mechanism for anisotropic etching of AlN and may produce relatively large features. On the other hand, ion beam assisted etching, or similar techniques, are likely to produces smaller features in these nitrides.

D. Future Research

The reactive ion etching system has been installed and will be used to etch GaN, AlN, InN and AlGaN on SiC substrates. In the preliminary stages of this research, several candidate materials (such as photoresist, NiCr, Al and other metals) will be tested in the various process gas streams to determine suitable masks for the etching process. In addition, experimentation with different cathode materials (such as graphite and quartz) is likely in order to minimize the amount of micromasking from the cathode material. Parametric studies will be conducted to determine how the power, pressure, gas load and flow rates affect the etching rate of these nitrides. Lastly, surface analysis techniques such as AES and XPS will be employed to determine the contamination levels and surface condition of the nitrides before and after etching.

E. References

1. *Plasma Processing of Materials: Scientific Opportunities and Technological Challenges*, National Research Council—Panel on Plasma Processing of Materials (National Academy Press, Washington, D.C., 1991).
2. J. W. Palmour, R. F. Davis, T. M. Wallett, K. B. Bhasin, J. Vac. Sci. Technol. A **4**, 590 (1986).
3. D. L. Smith, P. G. Saviano, J. Vac. Sci. Technol. **21**, 768 (1982).
4. D. L. Smith, R. H. Bruce, J. Electrochem. Soc. **129**, 2045 (1978).
5. C. J. Mogab, A. C. Adams, D. L. Flamm, J. Appl. Phys. **49**, 3796 (1978).
6. S. Matsuo, J. Vac. Sci. Technol. **17**, 587 (1980).
7. L. M. Ephrath, Solid State Technol., July 1982, p. 87.
8. Y. H. Lee, M. M. Chen, J. Appl. Phys. **54**, 5966 (1983).
9. L. M. Ephrath, J. Electrochem. Soc., August 1979, p. 1419.
10. A. J. vanRoosmalen, Vacuum **34**, 429 (1984).
11. M. Zhang, J. Z. Li, I. Adesida, E. D. Wolf, J. Vac. Sci. Technol. B **1**, 1037 (1983).
12. R. H. Bruce, G. P. Malafsky, J. Electrochem. Soc. **136**, 1369 (1983).
13. N. N. Efremow, M. W. Geis, R. W. Mountain, G.A. Lincoln, J.N. Randall, N.P. Economou, J. Vac. Sci. Technol. B **4**, 337 (1986).
14. S. Park, L. C. Rathburn, T. N. Rhodin, J. Vac. Sci. Technol. A **3**, 791 (1985).
15. H. F. Winters, J. Vac. Sci. Technol. B **3**, 9 (1985).
16. D. A. Danner, D. W. Hess, J. Appl. Phys. **59**, 940 (1986).
17. R. J. A. A. Janssen, A. W. Kolfschoten, G. N. A. vanVeen, Appl. Phys. Lett. **52**, 98 (1988).

18. Y. Ochiai, K. Shihoyama, T. Shiokawa, K. Toyoda, A. Masuyama, K. Gamu, J. Appl. Phys. **25**, L527 (1986).
19. G. Smolinski, R. P. Chang, T. M. Mayer, J. Vac. Sci. Technol. **18**, 12 (1981).
20. H. Tanaka, Optoelectron. Dev. Technol. **6**, 150 (1991).
21. J. S. Foresi, M.S. Thesis, Boston University, Boston, MA, 1992.
22. S. J. Pearton, C. R. Abernathy, F. Ren, J. R. Lothian, P. W. Wisk, A. Katz, Semiconductor Sci. Technol. **8**, 310 (1993).
23. I. Adesida, A. Mahajan, E. Andideh, M. A. Khan, D. T. Olsen, J. N. Kuznia, Appl. Phys. Lett. **63**, 2777 (1993).
24. S. J. Pearton, J. Vac. Sci. Technol. A **11**, 1772 (1993).
25. I. Akasaki, H. Amano, Physica B **185**, 428 (1992).
26. C. Eddy, Ph.D. Thesis, Boston University, Boston, MA, 1990.
27. T. Lei, T. D. Moustakas, J. Appl. Phys. **71**, 4933 (1992).
28. Z. J. Yu, B. S. Sywe, A. U. Ahmed, J. H. Edger, J. Electr. Mater. **21**, 782 (1992).
29. J. Sumakeris, Z. Sitar, K. S. Ailey-Trent, K. L. Moore, R. F. Davis, *"Layer-byLayer Epitaxial Growth of GaN at Low Temperatures"* (To be published in Thin Solid Films, 1993).
30. *CRC Handbook of Metal Etchants*, Eds. P. Walker, W. H. Tarn (CRC Press, Boca Raton, LA, 1991).
31. E. S. Dettmer, B. M. Romenesko, H. K. Charles, B. G. Carkhuff, D. J. Merrill, IEEE Trans. Comp. Hybrids Manuf. Technol. **12**, 543 (1989).
32. L. B. Rowland, Ph.D. Thesis, North Carolina State University, Raleigh, NC, 1992.
33. V. M. Donnelly, D. L. Flamm, Solid State Technol., April 1981, p. 161.

VIII. Distribution List

Mr. Max Yoder Office of Naval Research Electronics Division, Code: 314 Ballston Tower One 800 N. Quincy Street Arlington, VA 22217-5660	3
Administrative Contracting Officer Office Of Naval Research Resident Representative The Ohio State University Research Center 1960 Kenny Road Columbus, OH 43210-1063	1
Director, Naval Research Laboratory ATTN: Code 2627 Washington, DC 20375	1
Defense Technical Information Center Bldg. 5, Cameron Station Alexandria, VA 22314	2
Washington Headquarters Services ATTN: Dept. Acctg. Division Room 3B269, The Pentagon Washington, DC 20301-1135	2